Biogeosciences, 9, 317–340, 2012
www.biogeosciences.net/9/317/2012/
doi:10.5194/bg-9-317-2012

Biogeosciences

Fire, drought and El Niño relationships on Borneo (Southeast Asia) in the pre-MODIS era (1980–2000)

M. J. Wooster[1,2], **G. L. W. Perry**[3,4], **and A. Zoumas**[1]

[1]King's College London, Environmental Monitoring and Modelling Group, Department of Geography, KCL, Strand, London, WC2R 2LS, UK
[2]NERC National Centre for Earth Observation, UK
[3]School of Environment, University of Auckland, Private Bag 90219, Auckland, NZ
[4]School of Biological Sciences, University of Auckland, Private Bag 90219, Auckland, NZ

Correspondence to: M. J. Wooster (martin.wooster@kcl.ac.uk)

Received: 22 December 2010 – Published in Biogeosciences Discuss.: 7 February 2011
Revised: 15 December 2011 – Accepted: 19 December 2011 – Published: 16 January 2012

Abstract. Borneo (Indonesia) is Earth's third largest island, and the location of both extensive areas of rainforest and tropical peatlands. It is the site of both regular (seasonal) biomass burning associated with deforestation, land cover change and agricultural production preparations, and occasional, but much more severe, extreme fire episodes releasing enormous volumes of carbon from burning vegetation and peat. These extreme fire episodes are believed to result from anthropogenic practices related to (the still ongoing) forest degradation and clearance activities, whose impact with regard to fire is magnified by the effects of El Niño related drought. Since 2000, data from the MODIS Earth Observation satellite instruments have been used to study fire on Borneo, but earlier large fire events remain less well documented. Here we focus on a series of large fire episodes prior to the MODIS era, and specifically a 20 yr period covering both the two strongest El Niño events on record (1997–1998 and 1982–1983), along with an unprecedented series of more frequent, but weaker, El Niños. For the five El Niños occurring between 1980 and 2000, we develop quantitative measures of the fire activity across Borneo based on active fire counts derived from NOAA AVHRR Global Area Coverage (GAC) Earth Observation satellite data. We use these metrics to investigate relationships between the strength and timing of the El Niño event, the associated drought, and the fire activity. During each El Niño, we find areas of major fire activity confined within two or three fire sub-seasons (separated by monsoons) and focused in parts of South and Central Kalimantan, and sometimes also in East and/or West Kalimantan. For each El Niño we investigate various lag correlations, and find relationships of similar strength between monthly rainfall deficit and fire, but of more variable strength between indices of El Niño strength (ENSO indices) and rainfall deficit. The two strongest El Niño episodes (1982–1983 and 1997–1998) are accompanied by the most abundant fires (two and three times the active fire count seen in the next largest fire year), and the strongest correlations between measures of El Niño strength, rainfall and fire. We find the most significant positive statistical association between an ENSO index and fire activity to be that between the 16-month (first and second fire sub-seasons) cumulative NINO3 anomaly and the simultaneously recorded active fire count ($r = 0.98$, based on the five El Niño episodes between 1980 and 2000), although we find a negative association of equal strength between the cumulative NINO4 index and active fire count when considered over the entire two year duration of each El Niño episode (first, second and third fire sub-seasons). Our results confirm that the El Niño phenomenon, via its effect on precipitation, is a primary large-scale, short-term climatic factor that has a strong control on the magnitude of the fire activity resulting from the numerous land cover changes, agricultural preparation practices and human-caused ignitions occurring annually across Borneo. The results also suggest that ENSO forecasting maybe a realistic means of estimating the extent and magnitude of this fire activity some months in advance, thus offering some potential for forecasting effects on the remaining forest and peatland resource and the regional atmosphere.

Published by Copernicus Publications on behalf of the European Geosciences Union.

1 Introduction

Fire is a major driver of land cover change in many tropical forest areas, including Southeast Asia (Cochrane, 2003). In addition to the carbon stored in forest biomass, the approximately 250 000 km^2 of Southeast Asian peatland represents an immense reservoir of fossil carbon that is potentially combustible (Jaenicke et al., 2008; Couwenber et al., 2010; Page et al., 2009). The island of Borneo possesses more than 40 % of SE Asia's peatland, and is subject to ongoing land clearance, peatland draining and general forest degradation that over decades has resulted in large-scale transformations where natural ecosystems have been converted to degraded and managed cover types, resulting in a fragmented landscape with many anthropic ignition events. When such changes are accompanied by extreme drought, areas of normally moist peatland and forest can more easily dry, ignite and burn for weeks or months (Page et al., 2002, 2009; Goldammer, 2007). It is widely recognized that evidence of drought on Borneo extends back to the 19th century and beyond (e.g. Walsh, 1996). However, using visibility records from the region's airports, Field et al. (2009) demonstrated that large fire episodes commenced only in the 1980s, when population densities and forest exploitation on the island substantially increased, in part due to Government Transmigration Programs. Currently the population of Borneo is almost twice that of 1980, and Curran et al. (2004) show that between 1985 and 2001 the area of Kalimantan's protected lowland forests declined by more than 56 % (>29 000 km^2). These and other data support suggestions of strong links on Borneo between human population growth, forest exploitation, and fire occurrence (Goldammer, 2007), but drought promotes conditions conducive to the increased spread of fire into areas of degraded, and neighboring primary, forest; allowing the impact of anthropogenically driven fires to be further magnified. Since drought is not an annual occurrence on Borneo, fire activity on Borneo shows considerable interannual variability (van der Werf et al., 2006; Fuller and Murphy, 2006; Goldammer, 2007; Langner and Siegert, 2009; Miettienen et al., 2010). Fire activity peaks generally coincide with Pacific sea surface temperature enhanced "warm episodes", more commonly referred to as El Niño events, which typically occur every two to seven years and often result in significant rainfall deficits across all or part of the Island (Kousky and Higgins, 2007; Goldammer, 2007; Baker and Bunyavejchewin, 2009).

The largest fire events on Borneo in the late 20th century coincided with the 1997–1998 and 1982–1983 El Niño events, which are the strongest on record and known to be associated with significant drought on the island (Page et al., 2002; Jones and Cox, 2005; Ramonet et al., 2005). Over the last 25 yr a series of remote sensing studies have attempted to document the spatial and temporal patterns of these and other Indonesian fire episodes, particularly those occurring in El Niño years (e.g. Malingreau et al., 1985; Wooster et al., 1998; Legg and Laumonier, 1999; Wooster and Strub, 2002; Fuller and Murphy, 2006). A parallel set of studies has shown how fire activity in North and South America shows a strong relationship to climatological characteristics, such as sea surface temperature (SST) anomalies in the Pacific (largely related to the El Niño-Southern Oscillation; ENSO) and North Tropical Atlantic (e.g. Swetnam and Betancourt, 1990, 1998; Kitzberger, 2002; Alencar et al., 2006; Fernandes et al., 2011; Chen et al., 2011; Holz and Veblen, 2011). Such relationships provide information on the strength of the coupling between large fire episodes and climate characteristics, and have the potential to be used to forecast levels of fire activity many months in advance based on seasonal ENSO forecasting (e.g. Roads et al., 2001, 2005; Li et al., 2008; Jin et al., 2008; Barnston et al., 2010). If similar quantitative relationships linking climate and fire were available for Borneo, and other fire-affected parts of Southeast Asia, then the magnitude of the terrestrial and atmospheric impacts of the forthcoming fire season may be better anticipated and their effects forecast. For larger fire events, such effects include the potential for fire to spread into forest reserves and/or peatland stores of fossil carbon (e.g. Page et al., 2002, 2009), the release of globally-significant volumes of carbon dioxide and other greenhouse species (Simmonds et al., 2005); significant threats to already endangered forest fauna (including orangutans; Barlow and Silveira, 2009), and the development of regionally extensive areas of haze pollution (e.g. Heil et al., 2007; Goldammer, 2007). The extreme concentrations of particulates, polycyclic aromatic hydrocarbons, carbon monoxide, ozone and other hazardous species in this haze are believed to result in very significant human health impacts (Aditama, 2000; Emmanuel, 2000; Naeher, 2007), including at locations rather distant (e.g. Singapore) from the burning regions (Kunii et al., 2002; Aiken, 2004). Based on such forecasts, temporary controls on major land clearance activities, which are believed to be the foremost ignition source in the region, may even be considered (Langner et al., 2007). In this context, the purpose of the current work is to: (1) develop a quantitative record of levels of fire activity on Borneo covering El Niño episodes going back to the start of the 1980s, well before those of current active fire databases (e.g. those developed or used by Stolle et al. (2006), Langner and Siegert (2009), and van der Werf et al., 2006, 2008, 2010). In particular, the 20 yr period between 1980 and 2000 is unique in the satellite data record, as it captures an unprecedented series of rapid El Niño events and encompasses the two strongest El Niños on record (Trenberth and Hoar, 2006); and (2) to use this record to help elucidate the nature and strength of the empirical linkage between El Niño, drought and fire, for potential use in future forecasting efforts. Since this period is prior to the MODIS era, which began with the Terra satellite launch in December 1999, we use active fire (AF) measures derived from the extremely long-running NOAA Advanced Very High Resolution Radiometer

(AVHRR) Earth Observation sensor (Robel, 2009) as our fire activity metric.

2 Study area

2.1 Geography

Borneo (Fig. 1) is located on the equator, and is Earth's third largest island covering *c* 746 000 km^2. Together with Sumatra and Malaysia, Borneo possesses the world's highest concentrations of Dipterocarp forest ecosystems; these forests are drought-susceptible and, particularly following disturbance, vulnerable to fire (Guhardja et al., 2000; Seigert et al., 2001; Cochrane, 2003; Goldammer, 2007). Since the 1960s, large-scale exploitation has transformed much of the formerly forested lowlands of Borneo, including extensive peatlands, into agricultural plots, plantations, or degraded them via logging (Guhardja et al., 2000; Curran et al., 2004). The outcome is a highly fragmented landscape, within which there are numerous anthropogenic ignition events. If these ignitions coincide with periods of extremely low fuel moisture, related in particular to El Niño-related droughts, then fires can spread from heavily exploited areas into less disturbed forests and peatlands (Guhardja et al., 2000; Langner et al., 2007).

2.2 Climate

Borneo has an equatorial tropical climate, with often relatively light winds and only small annual temperature and humidity variations. Rainfall amounts are high in many areas (annual means exceeding 3000 mm) and show substantial seasonal variations (Hamada et al., 2002). Rainfall is characterized by a bi-modal monsoonal pattern, related to the north-south movement of the Intertropical Convergence Zone (ITCZ). A longer "wet" northeast monsoon is typical between November and March/April, and a shorter "dry" southwest monsoon between May/June and September/October (Langner et al., 2007). Aldrian and Susanto (2003) describe how rainfall regimes differ somewhat across the island of Borneo, with Eastern Kalimantan experiencing annual maximum precipitation in March–August, and Western Kalimantan in September–November (Hamada et al., 2002). Precipitation is generally highest in the northwest of the island and over the central mountainous regions, lower in the northeast and southeast, and lowest in the south and east coastal lowlands (Tapper, 1999; Kirono et al., 1999; Guhardja et al., 2000; Kirono, 2004). On inter-annual time scales, the ENSO is believed to be a major factor influencing Borneo's climate, most particularly rainfall, which can show strong deficits during major El Niños (warm ENSO events; Tapper, 1999; Haylock and McBride, 2001; Aldrian et al., 2007). The reverse is true during La Niña (cold ENSO) episodes, and as well as an overall reduction (increase) in precipitation during El Niño (La Niña), the rainy season onset typically comes later (earlier) in El Niño (La Niña) years (Hamada et al., 2002). While each warm ENSO event differs in its detail, these meteorological responses to El Niño are, for example, generally related to reductions/reversals in the normally easterly trade winds, ultimately resulting in the areas of heaviest convective rainfall normally present around Indonesia moving eastward across the Pacific. Related to this, warm water in the Western Pacific generally also moves eastward, and upwelling in the Eastern Pacific is reduced, resulting in significant increases in sea surface temperature (SST) across large regions of the ocean. Under "normal" (non-ENSO) conditions, SSTs range from 30 °C in the Western Pacific and 22 °C in the Eastern Pacific, but for example during the extreme 1997–1998 El Niño, positive SST anomalies exceeding 6 °C were recorded in some areas of the Eastern Pacific (see Fig. 1c). Kirono et al. (1999) indicate that during this event, virtually all of Indonesia experienced rainfall below the 10th percentile, with many stations recording the lowest rainfall on record. Gutman et al. (2000) used NOAA AVHRR data to dramatically illustrate the impact of this El Niño on Borneo's surface-atmosphere conditions.

The strength and phase (i.e. warm or cold phase) of an ENSO event is usually quantified via a simple index, historically based on measures of atmospheric pressure (i.e. the Southern Oscillation Index dating back to the end of the 19th century), but more recently via the average sea surface temperature (SST) anomaly measured over a fixed region of the tropical Pacific via satellite Earth observation and an observing network of buoy instruments (see Sect. 3.2 and Fig. 1c).

2.3 Fire

The palaeoenvironmental record provides evidence for recurrent periods of fire activity on Borneo over the Pleistocene and the Holocene, presumably as climatic oscillations (e.g. glacial-interglacial cycles and the ENSO) resulted in conditions favorable for fire (Goldammer, 2007). Fire activity seems to have intensified over the late Holocene (Page et al., 2009) and over the late 20th century fire has become an annual occurrence, its appearance being seasonal in nature and apparently closely coupled to spatio-temporal shifts in rainfall and changes in land cover (Goldammer 2007; Langner and Seigert, 2009). Studies of East Kalimantan (1978–1995) suggest that only El Niño-related rainfall deficits can account for the high fire danger indices seen during the El Niño years of 1982–1983, 1987, 1991–1992 and 1994 (Deeming, 1995; Fuller and Murphy, 2006). Furthermore, individual studies of different years using many types of satellite data record have already confirmed that it is these years of El Niño-related drought that are associated with the most extreme fire activity (e.g. Malingreau et al., 1985; Wooster and Strub, 2002; Fuller, 2003; van der Werf et al., 2006, 2008; Langner and Siegert, 2009). Goldammer (2007) suggests monthly rainfall totals below *c*. 100 mm, and two to three week periods

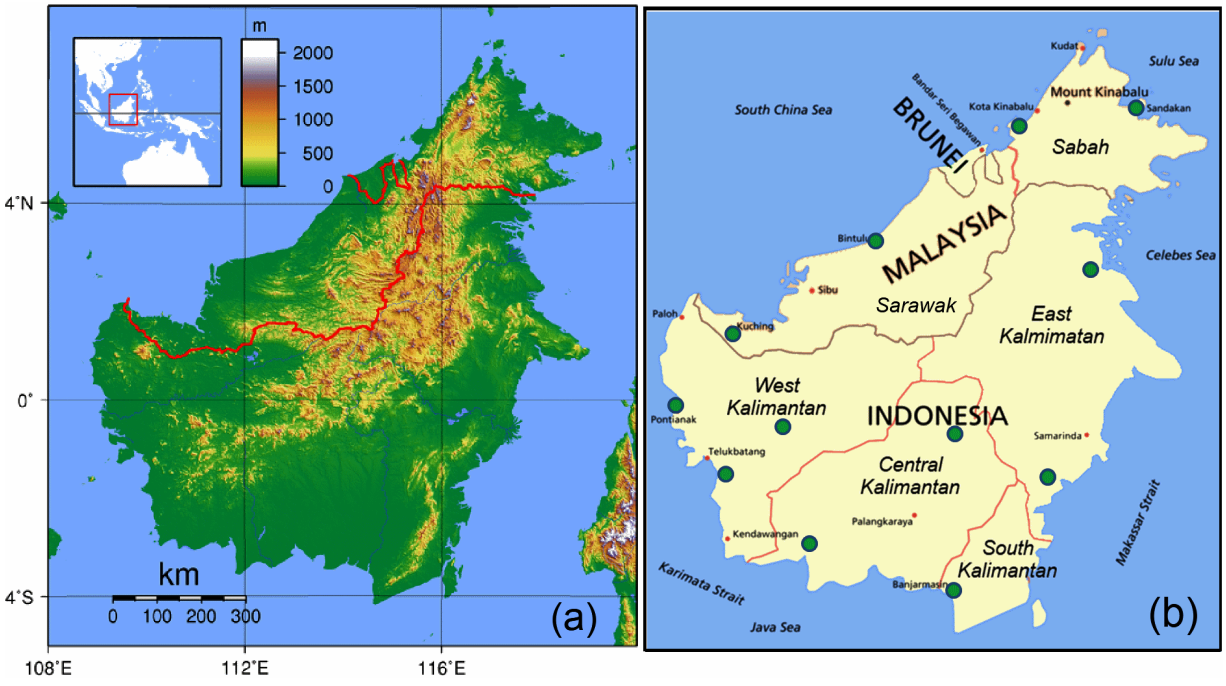

Fig. 1. Study area. **(a)** Island of Borneo, which contains territory of three countries; Malaysia (Sarawak and Sabah), Indonesia (Kalimantan) and Brunei, shown outlined. Kalimantan is further subdivided into the provinces of West, Central, East and South Kalimantan, as shown in **(b)**. Borneo is a mountainous island, with a dorsal range rising to a maximum elevation of 4101 m at Mount Kinabalu in the far northwest. The seven geographical regions of Borneo are shown outlined at right, and the circles highlight the location of the twelve meteorological stations whose rainfall records are compared to those of the NOAA Climate Prediction Centre Merged Analysis of Precipitation (CMAP) dataset (Xie and Arkin, 1996, 1997) used here. Towards the lowest lying coastal regions land cover is largely dominated by agricultural mosaics and peat swamp forest, with larger areas of evergreen lowland forest, degraded and/or regrowing forest becoming more prevalent towards the higher elevations (Langner et al., 2007). **(c)** Example of a sea surface temperature (SST) anomaly pattern seen during the development of an El Niño-Southern Oscillation (ENSO) event, in this case the extreme 1997–1998 El Niño. The upper (December 1997) SST anomaly map has the island of Borneo shown in **(a)** and **(b)** outlined, and also indicates the three regions of the tropical Pacific most commonly used for monitoring ENSO strength during both warm ENSO (El Niño) and cold ENSO (La Niña) conditions. All extend across the equator from 5° N–5° S, and NINO3 covers 90°–150° W, NINO4 150° W–160° E, and NINO3.4 120° W–170° W (Stenseth et al., 2002; Sarachik and Cane, 2010). These differing locations mean that the NINO3 region is situated within the "cold water tongue" that normally exists in the Eastern Equatorial Pacific, NINO4 lies on the edge of the Western Pacific warm-water pool, and NINO3.4 lies across both (Wyrtki, 1981; Kug et al., 2009). The widely used Operational Nino Index (ONI) is the three-month moving average of the NINO3.4 SST anomaly measure and is used by NOAA to formally designate months as showing El Niño or La Niña conditions (Smith, and Reynolds, 2003). The 1997–1998 ENSO event depicted in these SST anomaly maps reached El Niño conditions (defined by ONI>0.5 °C) in May 1997, and by December 1997 had peaked in strength (see Fig. 9). At this time, the normally easterly trade winds of the tropical Pacific had declined appreciably and/or reversed, warm water had spread in a major way from the Western Pacific towards the east (i.e. towards South America), and the upwelling and cold water tongue typical of the Eastern Pacific was very significantly weakened, with SST anomalies exceeding 6 °C in the easterly parts of the NINO3 region (note the SST anomaly scale in Fig. 1c extends only to +2 °C to best illustrate the size of the anomalous area, rather than its maximum). These changes resulted in SSTs exceeding 28 °C throughout the equatorial basin, with much warmer SSTs than normal across the entirety of the NINO3 and NINO3.4 regions and across the eastern part of NINO4, as seen in the first SST anomaly map for December 1997 (see e.g. Picaut et al., 2002 for a more detailed description). El Niño conditions persisted through March 1998 but were weakening (see March SST anomaly map), and finally ceased in June 1998 (see June SST anomaly map). Formal La Niña conditions (ONI<0.5 °C) developed the next month in July 1998 (see Fig. 9) and were characterised by a very rapid 8 °C decrease in SST in the equatorial region between 0° and 130° W (i.e. over the vast majority of the NINO3.4, and large parts of the NINO 3 and NINO4 regions) as described in Picaut et al. (2002). La Niña conditions lasted continuously until June 2000 (NOAA 2011a). All SST anomaly data mapped here are Global Ocean SST Anomalies, derived from data collected by the Tropical Rainfall Measuring Mission's (TRMM) Microwave Imager (TMI). TMI data shown here are produced by Remote Sensing Systems and sponsored by the NASA Earth Science MEaSUREs DISCOVER Project. Microwave OI SST data are produced by Remote Sensing Systems and sponsored by National Oceanographic Partnership Program (NOPP), the NASA Earth Science Physical Oceanography Program, and the NASA MEaSUREs DISCOVER Project. Both datasets are available at www.remss.com.

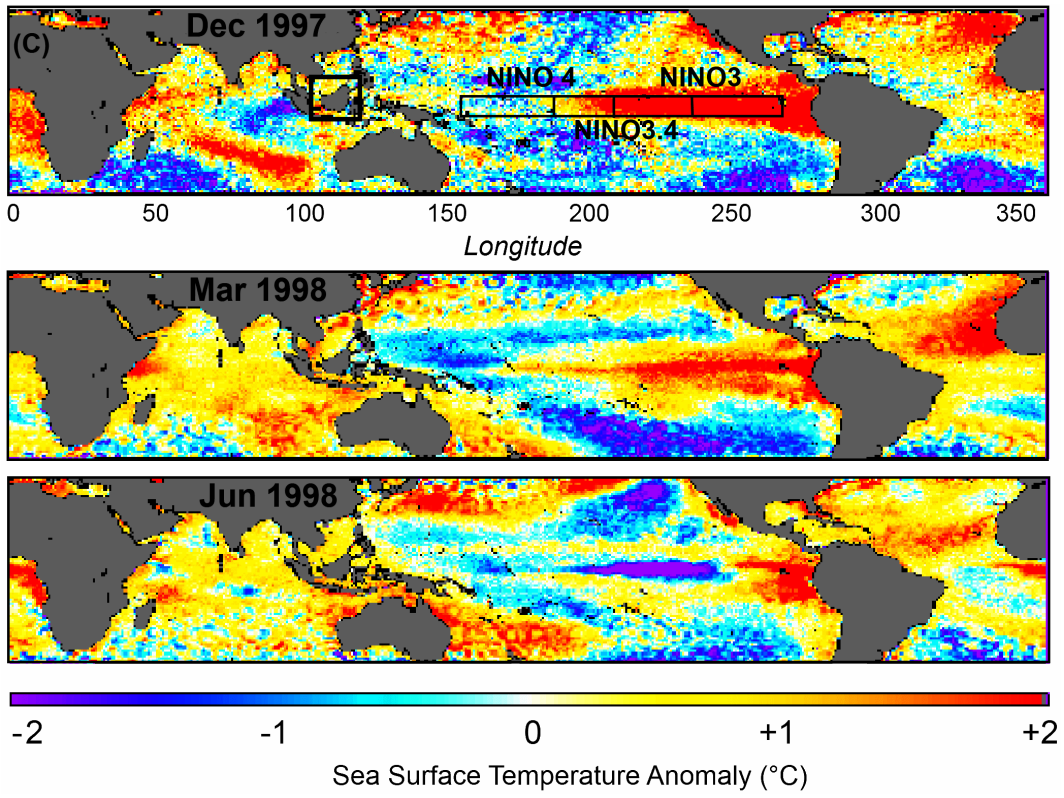

Fig. 1. Continued.

without rain, as a potential critical threshold with regard to the development of large fire conditions driven by human ignitions and exacerbated by El Niño related drought. There is anecdotal evidence extending back to the 1880s of significant forest mortality during such droughts, although interestingly these reports do not mention fire (Goldammer, 2007). Field et al. (2009) suggest that large fire episodes only began in the 1980s as forest exploitation by humans increased. During more recent El Niños, large fire events have become commonplace, though drought, *per se*, may cause as significant an amount of tree mortality and biomass reduction in the affected forests as do the associated fires (van Nieuwstadt and Sheil, 2005). It is clear that there are strong links between El Niño events, drought and fire on Borneo. Indeed, over the period 1996–2003, Schultz et al. (2008) demonstrated a strong correlation between total annual (remotely sensed) fire pixel count and integrated ENSO index strength, showing how fire activity peaked during the 1997–1998 El Niño. However, the empirical nature and strength of relationships between El Niño, drought and fire on Borneo has yet to be fully determined, certainly for the El Niños we consider here, which largely pre-date the times of existing active fire datasets and analyses (e.g. Fuller and Murphy, 2006; Schultz et al., 2008; Langner and Siegert, 2009).

3 Datasets

3.1 Satellite active fire detections

Infrared (IR) observations from Earth orbiting satellites provide spectral radiance and brightness temperature (BT) measures that at some wavelengths are very sensitive to the radiant energy emissions from even highly sub-pixel fires, particularly so at middle infrared (3–5 µm) wavelengths (Robinson, 1991). To be most useful these MIR measurements must be accompanied by longwave IR (LWIR; 8–12 µm) observations that help to minimise "false alarms" from areas of warm, bare ground and for cloud masking (Zhukov et al., 2006). By day, VIS/NIR measurements (0.4–1.1 µm) are also a useful addition, particularly for screening out areas affected by sunglint (Giglio et al., 2003a; Xu et al., 2010). The MODIS sensor flying on the EOS Terra and Aqua satellites (launched in 1999 and 2002) currently provides probably the most commonly used active fire observations, with records extending from 2000 and 2002, respectively). These "Active Fire and Thermal Anomaly" products (MOD14 and MYD14; Giglio et al., 2003a) have provided a regular, well-characterised global record of active fires since 2000. A series of spatio-temporal studies aimed at elucidating patterns of fire activity and their interannual variability have been based on these MODIS products (e.g. Giglio et al.,

2006; Chuvieco et al., 2008; Ichoku et al., 2008), including studies focusing explicitly on Borneo and which combine these records with those from other Earth Observation systems (e.g. Fuller, 2003; Simmonds et al., 2004; Langner and Siegert, 2009).

In contrast to post-2000 studies, the long-standing Advanced Very High Resolution Radiometer (AVHRR) provides the data source for the current study, which focuses on fire activity on Borneo during the 1980s and 1990s. Prior to the MODIS-era, the AVHRR provided the majority of data for studies of active fires (Robinson, 1991), and was carried by NOAA's Polar Orbiting Environmental Satellite (POES) series. The most recent launch of an AVHRR was onboard the NOAA-19 POES satellite in February 2009, and the newest version of the sensor (the AVHRR/3) is now also carried onboard the European MetOp satellites (Edwards et al., 2006).

A single AVHRR swath is *c*. 2400 km wide, and raw "Local Area Coverage" (LAC) format AVHRR data has a 1.1 km spatial resolution at nadir, very similar to that of MODIS. Figure 2 illustrates three typical AVHRR LAC scenes from Southern Borneo collected during the fire seasons of three climatologically different years; (a) the 1997 El Niño, (b) the 2001 "normal" year, and (c) the 1999 La Niña. Pixels containing actively burning fires appear black in this rendition, and the greatly increased fire activity during the El Niño year (a) when compared to the "normal" year (b), and the further reduced number of fires seen during La Niña conditions (c), is typical of AVHRR scenes we examined. Our analyses of these and other LAC scenes confirm previous conclusions that AVHRR data are very suitable for the detection and characterisation of gross variations in fire activity in this tropical environment (e.g. Fuller and Fulk, 2000; Siegert and Hoffmann, 2000; Langner and Siegert, 2009).

While LAC data are the optimum data source for AVHRR-based active fire studies, unfortunately this full spatial resolution data format was not routinely archived by NOAA at a global scale due to onboard data storage limitations of the POES system. This limitation has been removed for the more recent MetOp satellite series, but for many areas outside of the continental USA, the historical NOAA POES AVHRR LAC data coverage is infrequent, and NOAA's central repository for AVHRR data (the online CLASS database; http://www.class.noaa.gov) indicates that Indonesia is quite sparsely covered. Regular (daily) coverage by AVHRR is, however, available globally via a reduced spatial resolution version of the original 1 km AVHRR data record, termed the Global Area Coverage (GAC) AVHRR data product. The pixel averaging and pixel/line skipping procedures used to derive the spatially sub-sampled GAC data from the original AVHRR LAC observations are conducted onboard the POES satellite as the data are collected, according to the procedures detailed in Robel (2009) and described, for example, in Wooster and Strub (2002). The resultant GAC data record is sufficiently low volume (1/16th of the original LAC data) that it can be continuously recorded until the POES satellite is within site of a US data-down link station, and thus a global GAC data record exists back to the early years of POES operations.

Each AVHRR GAC pixel can be considered as representing the spectral radiance signal from a 4.4×1.1 km area (at nadir), with a 3.3 km gap between each scan line of data. Despite these unusual spatial characteristics, AVHRR GAC data processed through standard fire detection algorithms have been used to document variations in fire activity (e.g. Koffi et al., 1996). Indeed, in the pre-MODIS era, the only alternatives to using GAC data to derive global active fire datasets based on MIR and LWIR channel observations are the ERS-2 ATSR and Tropical Rainfall Measuring Mission (TRMM) VIRS sensors, whose active fire products are described in Schultz (2002) and Giglio et al. (2003b), respectively. However, while both the ATSR and VIRS sensors possess a similar set of spectral bands to AVHRR, they have significantly narrower swaths (ATSR: 512 km; VIRS: 720 km), meaning that a single scene is insufficient to cover the whole of Borneo and this limits their temporal frequency (e.g. Mota et al.,2006). Furthermore, the ATSR and VIRS datasets extend back only to the 1996 and 1998 fire seasons respectively, only a few years earlier than the start of the MODIS record. In contrast, AVHRR GAC data completely cover Borneo in a single scene, and are available back to the 1982–1983 extreme El Niño episode, so we focus our study on this data record. However, raw GAC data for Borneo is not routinely processed into active fire detection products, so we undertook this processing for the analyses presented here. The alternative, but shorter-duration, ATSR and TRMM AF datasets can thus be used to evaluate the robustness of our GAC-derived AF data record during overlapping time-periods, and because TRMM provides observations with a varying local overpass time it allows important information on the fire diurnal cycle to be derived (Giglio, 2007).

Using AVHRR-derived active fire data of Borneo, Malingreau et al. (1985) and Wooster et al. (1998) illustrated the extreme magnitude of Borneo's 1983 and 1997 fire activity, respectively, and Wooster and Strub (2002) demonstrated that variation in fire activity could be quantified using AVHRR GAC data over the period of the extended 1997 El Niño-related drought. Figure 3 shows an example of matching AVHRR LAC and GAC data collected during the 1997 El Niño, indicating that the signature of active fires is clearly evident in the GAC data record. Here, therefore, we focus on using GAC data to construct a robust and reliable multi-year active fire dataset for Borneo covering five El Niño events (1982–1983 to 1997–1998), in order to allow quantitative comparisons of fire activity with the climatic conditions (e.g. rainfall deficits) believed to be strong regional drivers of fire. We obtained raw GAC imagery from the NOAA CLASS database, calibrated it using the procedures outlined in Wooster et al. (2005) and Robel (2009), and applied a simple but effective active fire detection algorithm

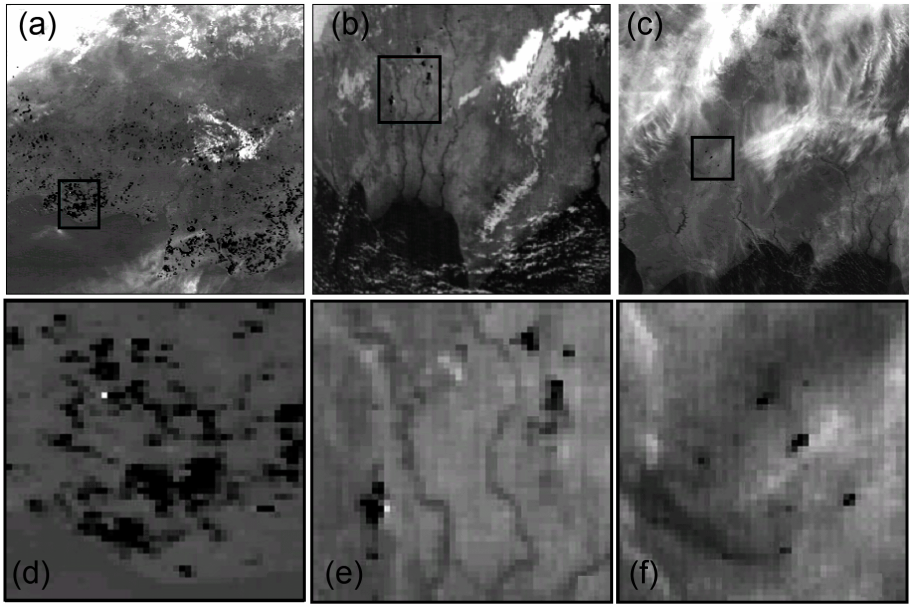

Fig. 2. Raw night-time AVHRR Local Area Coverage (LAC: 1.1 km spatial resolution at nadir) imagery of the coast of Central Kalimantan. Data shown are image subsets from the AVHRR 3.7 µm channel, with boxed areas shown magnified beneath. Data were collected during **(a)** El Niño (21 October 1997), **(b)** "normal" (6 September 2001) and **(c)** La Niña (29 July 1999) climatological episodes. Each top-row image covers an area of around 300 × 300 km, and the Java Sea can be seen towards the bottom of each image subset. The AVHRR 3.7 µm channel is highly sensitive to active fires, with increased pixel radiances resulting even from highly sub-pixel events (Robinson, 1991). Such fire affected pixels show elevated 3.7 µm channel spectral radiances (due to the intense fire thermal emissions in this wavelength range), and appear black in this rendition. Meteorological clouds typically show low 3.7 µm channel spectral radiances at night (due to their low temperatures), and appear white in this rendition. Active fire pixels can be seen in each scene, but their number decreases substantially when you move from "El Niño" to "normal" and then to "non El Niño" conditions. Different image dates are necessarily shown in each year to the relative scarcity of AVHRR LAC images over Borneo (see Sect. 3.1), but the selected images depict typical examples of the fire situation for each of the three climatological conditions. Data shown are raw AVHRR LAC imagery, uncalibrated and not geometrically corrected.

previously demonstrated to be capable of quantifying fire activity on Borneo (Wooster and Strub, 2002).

3.2 ENSO indices

El Niño events vary in their evolution, intensity, duration, and climatic teleconnection patterns (Kitzberger, 2002; Kug et al., 2009). The regional effects of each El Niño also vary, depending on how their specific characteristics interact with the normal atmospheric circulation patterns (Simard et al., 1985). The monthly strength of an ENSO event is typically quantified using an ENSO index, or derived metric. NINO-X indices are based on Pacific Ocean sea surface temperature (SST) anomaly measures (Fig. 1c), with "X" denoting the particular area of the ocean used (e.g. NINO3.4 being the mid-tropical Pacific; Stenseth et al., 2002; Sarachik and Cane, 2010). Different ENSO events may affect the SST anomaly measures of different regions of the Pacific to varying degrees, but by whatever measure the 1982–1983 and 1997–1998 El Niños are considered by far the strongest on record (Wolter and Timlin, 1998). In addition to the NINO-X indices, our study also makes use of the Operational Nino Index (ONI), which represents the three-month moving average of the NINO3.4 SST anomaly measure (Smith, and Reynolds, 2003) and is used by NOAA to classify months as showing El Niño conditions or not (Kousky and Higgins, 2007).

We obtained ENSO indices for the years 1980–2000 from the NOAA Climate Prediction Centre (NOAA, 2011a), a period within which five El Niño events occurred. We term these events as 1982–1983, 1986–1987, 1991–1992, 1993–1994 and 1997–1998 (Sarachik and Cane, 2010). Other studies have confirmed these as the years where fire activity was elevated across large parts of Indonesia (e.g. Malingreau et al., 1985; Wooster and Strub, 2002; Dennis, 1999; van der Werf et al., 2006; Langner and Siegert, 2009; Baker and Bunyavejchewin, 2009). Although each of these El Niño events is nominally stated to occur over a two year period (i.e. ENSO Year 1 and ENSO Year 2), we also use NOAA's formal definition that a month's ONI index must exceed +0.5 °C for it to be included in an El Niño event; and that this threshold must be meet for a period of at least 5 consecutive months for a significant episode to be recognised based on the ONI metric (Kousky and Higgins, 2007; NOAA, 2011a). Table 1

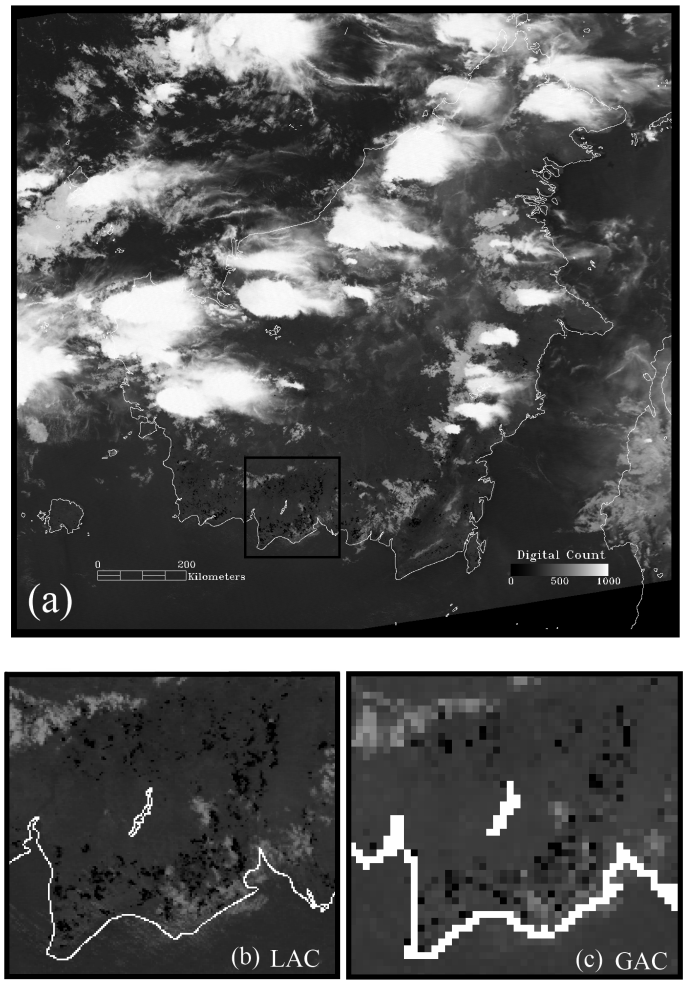

Fig. 3. Matching nighttime AVHRR 3.7 µm channel LAC and GAC data of Borneo taken on 12 October 1997 during the height of the El Niño episode when many fires were burning, particularly along the coast of Central Kalimantan (Wooster and Strub, 2002). Data are shown in an uncalibrated form to aid interpretation, resulting in high radiance (i.e. low AVHRR digital count) fire pixels appearing black in this rendition. A raster coastline is superimposed on the imagery to outline the island of Borneo. Plate **(a)** shows the full AVHRR LAC scene of Borneo, with the most heavily fire-affected area outlined in black. This area is shown magnified in the LAC and matching GAC data subsets shown as **(b)** and **(c)** respectively. Despite the GAC sampling and pixel averaging process, the low digital count fire pixels are seen in both LAC and GAC data formats. Data are shown geometrically corrected to aid the visual comparison.

lists the months classified as being part of an El Niño episode based on these ONI criteria.

Forecasting of ENSO indices based on modelled equatorial SST anomalies has gained increased attention in recent years, and is now relatively routine. Jin et al. (2008) indicate that tier-1 multi-model ensemble (MME) forecasts of NINO3.4 SSTs now have an anomaly correlation coefficient of 0.86 at a six month lead time. Though we do not use ENSO forecasts here, such predictability means that any significant relationships we discover between El Niño, drought and fire could potentially be driven by ENSO forecasts in order to deliver prior warning of enhanced fire conditions.

3.3 Rainfall

The large-scale temporal pattern of Indonesian rainfall is almost exclusively controlled by the monsoon, resulting in discrete wet and dry seasons (Kirono et al., 1999). On Borneo, El Niño episodes tend to significantly reduce the amount of monsoonal rainfall, although it never fails completely (Kirono et al., 1999; Guhardja et al., 2000). To quantify trends in rainfall we used the monthly NOAA Climate Prediction Centre Merged Analysis of Precipitation (CMAP) rainfall dataset (NOAA 2011b), which is gridded to 2.5° latitude × 2.5° longitude and extends back to 1979. The CMAP data are derived from merging precipitation measures from several IR- and microwave-based satellite rainfall estimates

Table 1. ENSO index data for the five El Niño episodes examined herein (1982–1983, 1986–1987, 1991–1992, 1993–1994 and 1997–1998).

					Time integrated ENSO index (°C-months); NINO3/NINO3.4/ONI		
ENSO Event	Months officially classed as El Niño *	Max NINO3 Anomaly (°C)	Max NINO3.4 Anomaly (°C)	Max ONI (°C)	Including all ENSO Year1 and Year 2	Including first 16 months only	Including months listed in Column 2
1982	May 1982				27.22	23.16	26.50
to	to	2.8	3.3	2.3	18.45	20.41	21.69
1983	June 1983				16.79	18.27	19.31
1986	August 1986				15.02	4.41	18.23
to	to	1.7	1.8	1.6	17.35	6.31	21.23
1987	Feb 1988				18.75	8.03	20.97
1991	May 1991				11.02	10.77	12.67
to	to	1.4	1.9	1.8	15.50	14.43	15.37
1992	July 1992				18.65	15.96	16.96
1993	May 1994				4.88	3.24	−1.69
to	to	1.1	1.3	1.3	9.32	4.53	1.61
1994	March 1995				13.18	6.77	9.21
1997	May 1997				25.45	29.20	31.91
to	to	3.6	2.7	2.5	13.23	21.86	23.39
1998	May 1998				16.16	21.75	22.62

* Based on the ONI≥0.5 °C threshold. For historical purposes, based on this metric warm (El Niño) and cold (La Niña) ENSO episodes are defined only when this threshold is met for a minimum of 5 consecutive months; see NOAA (2011a) for a full tabulated ONI record.

with rain-gauge data (Xie and Arkin, 1996, 1997). For comparison to the CMAP datasets we used two other rainfall measures: (1) v6 of the daily 3B42 rainfall measure derived at 0.25° latitude × 0.25° longitude from Tropical Rainfall Measuring Mission (TRMM) satellite observations, which extends back to 1997 (Huffman et al., 1997; NASA, 2011), and (2) a series of monthly rainfall totals from twelve meteorological stations distributed across Borneo as shown in Fig. 1b.

4 Methodology

4.1 Derivation of active fire metrics

4.1.1 Observation time

Fire activity generally shows a strong diurnal cycle (Roberts et al., 2010), and in most tropical regions fire activity peaks during the afternoon (Giglio, 2007). For many investigations therefore, metrics based on daytime active fire detections are preferred since fire numbers are maximised, although these datasets may show a greater frequency of false alarms due to the presence of solar-heated bare ground and/or sunglints from unmasked water bodies or clouds (Robinson, 1991). Fire detection algorithms attempt to minimise daytime false alarms by using multi-spectral methods to separate sunglints and homogenously warm surfaces from active fires (Zhukov et al., 2006), however Wooster and Strub (2002) found that this discrimination is much more difficult to accomplish using the spatially averaged GAC data. Some previous AVHRR-based active fire studies have relied on nighttime active fire data records (e.g. Langaas, 1993; Legg and Laumonier, 1999), and indeed the ATSR World Fire Atlas (Schultz, 2002; Mota et al., 2006) that is exploited in the widely used Global Fire Emissions Database (van der Werf et al., 2006, 2010) is also a nighttime-only product. Difficulties with identifying daytime false alarms in GAC data, coupled with the fact that sunset on Borneo occurs at the relatively early time of 18:00 hr ± 30 min, when fire activity might still be quite strong, suggested that GAC data taken during the early nighttime period may be quite suitable for our study. To confirm this, we compared AF detections derived from eleven matched daytime (14:30–15:30 hr LT) and nighttime (18:30–19:30 hr) GAC image pairs, based on data from the 1991–1992 and 1997–1998 El Niño events. With this small test dataset, unlike for our subsequent multi-year study which used many hundreds of images, we could manually screen the daytime datasets for sunglint-induced false alarms. Figure 4 illustrates a strong, linear relationship between the daytime and corresponding early nighttime active fire counts, suggesting that AF metrics based on early nighttime GAC observations are of a similar efficacy to those derived via carefully screened daytime observations. In fact, perhaps surprisingly, in most cases we found that the AF counts derived from the early night-time scenes were actually higher than those in the daytime scenes, and the reason for this is explored further in Sect. 4.1.2.

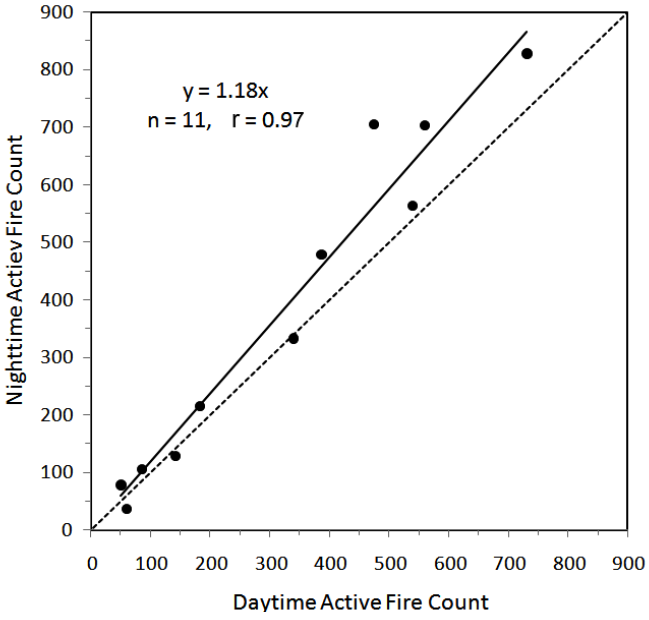

Fig. 4. Comparison of nighttime and daytime active fire counts derived from the type of AVHRR GAC data of Borneo shown in Fig. 3c. Each point represents the number of active fire pixel counts derived for the same day from AVHRR GAC data coverage made at two different times of day. Daytime scenes were collected between 14:30 and 15:30 hr, and nighttime scenes between 18:30 and 19:30 hr LT. Scenes were collected during the 1991–1992 and 1997–1998 El Niño episodes, and a significant positive correlation can be seen between the active fire count numbers measured at the two different overpass times. Perhaps somewhat surprisingly, the best-fit linear relationship (black line) indicates that nighttime active fire count numbers are typically higher than the matching daytime active fire count numbers. The 1:1 line is also shown (dashed line).

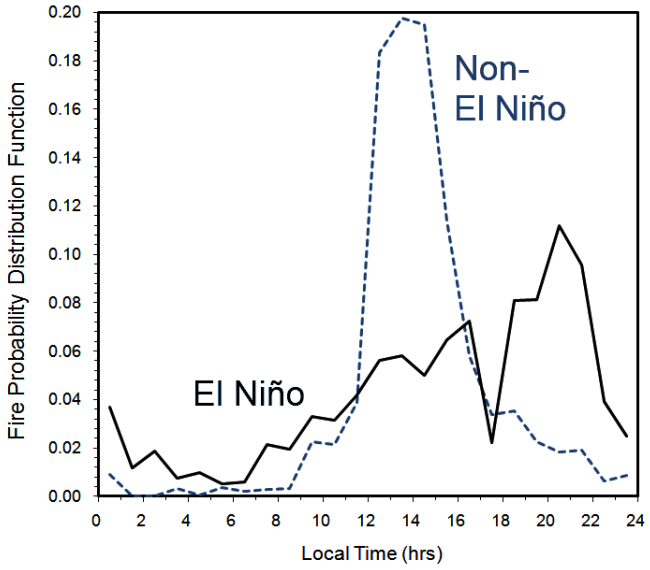

Fig. 5. Fire diurnal cycle in Borneo during El Niño and non-El Niño periods, as derived from TRMM VIRS active fire data (Giglio, 2007). During non-El Niño periods (1999–2001), the majority of fire activity is centred on a relatively short period between noon and 16:00 hr LT, while during an El Niño period (1998) the fire diurnal cycle appears significantly damped, with the peak shifted towards early night-time (∼21:00 hr).

4.1.2 Normalisation for orbital drift

Although we focus on active fire detections in early nighttime AVHRR GAC data, a further consideration with regard to any multi-year active fire dataset is the potential for orbital variations to impact the active fire metrics through its interaction with the diurnal fire cycle. Since each NOAA POES satellite typically remains the operational satellite for a maximum of five years, by necessity over the period of our study the AVHRR GAC data come from a series of POES systems, starting from NOAA-7 and extending to NOAA-12. The local overpass times of these satellites is not constant, and drifts by around one or two hours over the nominal three or four year lifetime of each satellite mission (Price, 1991). The interplay between this drift and the fire diurnal cycle may introduce bias into any AVHRR-derived multi-year AF record. To investigate this, information on Borneo's diurnal fire cycle was extracted from the TRMM VIRS AF record described by Giglio (2007) and is shown in Fig. 5. During non-El Niño periods, fires in Borneo were confirmed as showing a strong diurnal cycle typical of tropical regions, with fire activity concentrated in the early afternoon and for a relatively short duration. However, during El Niño conditions the fire diurnal cycle appears strongly damped, with fires being more evenly distributed across the day, possibly as a result of the increasingly dry and flammable fuel conditions resulting from drought. Under these conditions, AF counts made by TRMM VIRS actually peak in the early evening; this also explains why our GAC-derived AF counts were often higher under these conditions than during the day (i.e. as seen in Fig. 4). Using the El Niño fire diurnal cycle information derived from TRMM VIRS dataset (i.e. that shown in Fig. 5), we normalised our AVHRR GAC-derived AF counts for the effect of variations in the local overpass time of the NOAA POES satellites.

4.1.3 Selection of observation years

Figure 2a illustrates the severe nature of fire activity on Borneo during the 1997 El Niño, and Fig. 3 confirms that under these conditions AVHRR GAC data identifies active fire pixels, despite the spatial subsampling and pixel averaging involved in the dataset's generation.

To investigate whether fires could be discriminated under other climatological conditions, a series of matching LAC and GAC images were obtained for both El Niño and non-El Niño years, and a version of the AVHRR GAC active fire detection algorithm described in Wooster and Strub (2002)

applied to both. There is a strong and linear relationship between active fire counts derived from the LAC and GAC versions of the same AVHRR data during the 1997 El Niño period ($r = 0.99$, $n = 13$: Fig. 6a). When the same comparison is conducted for La Niña and "normal" years (19 scenes from 1995, 1999, 2000 and 2001) a weaker relationship is found ($r = 0.88$, $n = 19$), although active fire pixel numbers are typically an order of magnitude or more lower at these times than during El Niños (cf. Fig. 2). The weaker relationship between the LAC and GAC active fire counts during non-El Niño periods is due to the AF pixels radiating more weakly and being more spatially isolated under these climatic conditions (Fig. 2b, c). Under such non-optimal burning conditions, the subsampling and line skipping procedures used to derive the GAC data cause many of the active fires present in the LAC scene to fail to result in a matching GAC AF pixel detection. Thus, we limit our analysis to the five El Niño episodes occurring between 1980 and 2000, which, in any case, represent the periods of maximum fire activity on Borneo over the study period (Langner and Siegert, 2009). For each of these events we analysed many GAC scenes for each month of each El Niño episode, fully covering ENSO Year 1 and ENSO Year 2. For the 1986–1987 and 1993–1994 El Niño events we also analysed GAC data of the first few months of 1988 and 1995, since for these events El Niño conditions are considered to have persisted into ENSO Year 3 based on the ONI $\geq$+0.5 °C criteria (Table 1).

For the full 24+ months of each El Niño event, we selected numerous nighttime AVHRR GAC scenes from the NOAA CLASS database and processed them with an adaptation of the Wooster and Strub (2002) algorithm in order to derive our active fire (AF) data record. Scene selection was based on: (1) Borneo lying towards the centre of the AVHRR swath (to deliver the highest spatial resolution and minimum level of geometric distortion), and (2) minimal cloud obscuration of the island, particularly in the coastal regions which are the locus of fire activity (Fuller and Fulk, 2000; Langner and Siegert, 2009). Scenes failing to meet these criteria were either identified at the online "quicklook" stage (i.e. were not downloaded), or were downloaded but were removed during initial data screening. The resulting multi-year AF record was based on a mean ($\pm 1\sigma$) of 120 ± 15 scenes per year, with typically 5–10 scenes per month processed for the main fire periods.

4.1.4 Normalisation for cloud cover

Although active fires can be readily detected through smoke, the obscuring effects of cloud cover generally require that fire pixel counts be normalised for inter-scene variations in cloudiness if they are to be used to quantify temporal changes (e.g. Heald et al., 2003; Schroeder et al., 2007). Given Borneo's tropical climate and thus relatively high land surface-temperature, cloud detection by night is reasonably easy to perform using brightness temperature thresholding, for example of the AVHRR 11 µm channel data (Kaufman et al., 1990). Fortunately, in terms of cloud obscuration, the climatological shifts experienced during El Niño make cloud cover far less of a problem than would be the case in non-El Niño years, when some areas of Borneo are almost continuously obscured (Langner et al., 2007). Nevertheless, cloud cover is still a significant feature of Borneo, and our AF dataset therefore required adjustment for inter-scene cloud cover variations. The normalisation procedure is based on the assumption that fire occurrence across a region is spatially uncorrelated with cloud-cover (as per Kaufman, 1990; Giglio et al., 2003b; Heald et al., 2003). In fact, the majority of Borneo's fire activity occurred in coastal areas, as opposed to the more mountainous and cloud-affected interior (Fig. 1a), and preliminary analyses suggested that fire activity was not temporally metasynchronous across Borneo, typically peaking, for example, between August and October in South and Central Kalimantan, but between February and April in East Kalimantan. Because of this spatial-and temporal asynchronicity, cloud-normalisation was not conducted on an island-wide basis, but rather AF detections made in each of Borneo's seven geographic regions (Fig. 1b) were normalised by the percentage of cloud cover in that same region. The total island-wide AF pixel count, normalised for both satellite overpass time and cloud cover variations, was then derived by aggregating these adjusted fire counts.

4.1.5 Comparison to ATSR world fire atlas fire product

Our multi-year active fire record for Borneo, normalised for temporal variations in both satellite overpass time and cloud cover, covered the 1982–1983, 1986–1987, 1991–1992 and 1993–1994 and 1997–1998 El Niño events. The majority of these El Niño episodes on Borneo have not been previously examined in terms of their AF spatio-temporal metrics. To evaluate the efficacy of our AF data record, GAC-derived AF counts for Borneo for the 1997 El Niño were compared to those from the ATSR World Fire Atlas (which is employed in the Global Fire Emissions Database of van der Werf et al., 2006, 2010). Both the GAC and ATSR active fire records indicate that the vast majority of fires burning during 1997 occurred in Central and East Kalimantan, and a strong agreement is seen between the temporal pattern depicted in the two different datasets (Fig. 6b).

4.2 Comparison of trends in El Niño, rainfall and fire

4.2.1 Derivation of rainfall information

The CMAP dataset (NOAA, 2011b) was used as the primary rainfall dataset for comparison to the monthly active fire count data. The CMAP data were subset into two area-averaged versions, one based on the 2.5° grid cells that

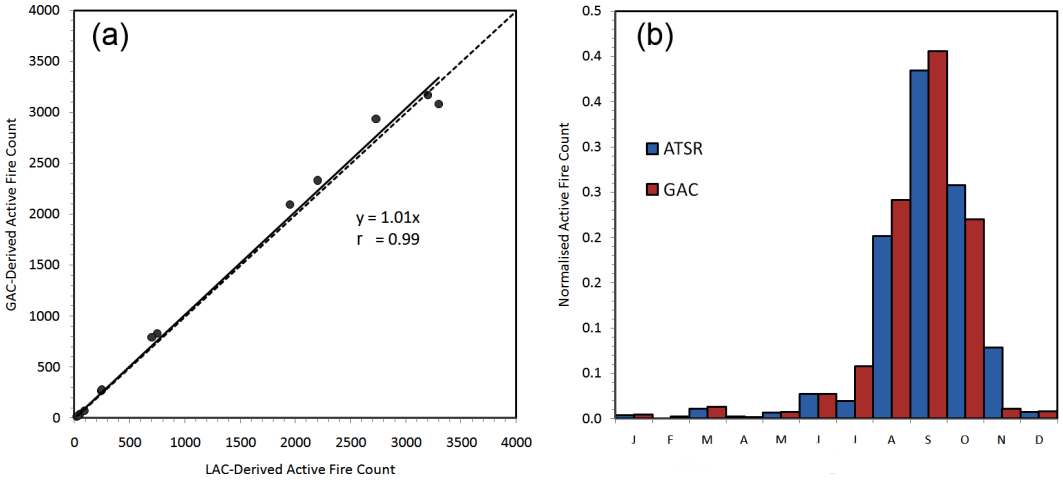

Fig. 6. Comparison of the active fire (AF) pixel count for Borneo derived for the 1997 El Niño period. **(a)** Comparison between AF pixel counts derived from GAC and LAC versions of the same thirteen AVHRR scenes (examples of which are shown in Fig. 3b and c). The 1:1 line is also shown. **(b)** Temporal trend in the normalised AF pixel count for the 1997 El Niño period, derived via the AVHRR GAC processing described herein and from the widely used ATSR World Fire Atlas (Schultz, 2002; Mota et al., 2006). Strong similarities are evident in all cases.

covered all of the island of Borneo ("all Borneo"), and one based on those covering only Borneo south of the equator (since this is the region apparently most affected by fire, see e.g. Fig. 3; "Southern Borneo"). Comparison with averaged monthly rainfall totals for the years of overlap for the twelve meteorological stations shown in Fig. 1b showed a strong correlation between the station average monthly rainfall and the all and Southern Borneo area-averaged CMAP data ($r =$ 0.98 and 0.88, respectively). Comparison between the same CMAP data and the overlapping TRMM 3B42 v6 rainfall measure also showed a strong correlation ($r = 0.98$ for both the "all Borneo" and "Southern Borneo" CMAP measures). Having established the efficacy of the CMAP rainfall data, the two area-averaged CMAP rainfall measures were used to calculate the monthly "all-Borneo" rainfall deficit (ABD) and "Southern-Borneo" rainfall deficit (SBD) via a comparison to corresponding long-term (1979–2009) means.

4.2.2 El Niño-rainfall-fire intercomparison methods

At a monthly time-step, temporal trends in Borneo's active fire counts were compared to the metrics derived from the two CMAP-derived rainfall measures and to the ONI, NINO3 and NINO3.4 indices collected from the NOAA Climate Prediction Centre (NOAA, 2011a). To evaluate the temporal relationship between ENSO index, drought and fire occurrence, we used cross-correlation techniques (similar to Fuller and Murphy, 2006); we limited consideration to negative lags as we were interested solely in the effects of El Niño and rainfall deficit leading to (i.e. preceding) fire activity variations. We explored temporal associations between the ENSO index (ONI and ENSO-X) anomalies and (1) rainfall deficit, and (2) fire activity. We calculated cross-correlations between ENSO-X (NINO3 and NINO3.4) and ONI index anomalies, rainfall deficits and fire activity over: (1) the full 24 month fire periods and (2) only for those months during each period when the ONI exceed 0.5 °C (with a three-month buffer for the cross-correlation analysis). For the ENSO-X indices we correlated the index anomaly with the monthly fire count, but as the ONI is a three-month average we correlated it with a three-month running mean of fire counts. The length of the time-series precluded formal pre-whitening (Chatfield, 1995), but the use of ENSO index anomalies and rainfall deficits removes some of the seasonal trend from these data. Analyses were conducted in R-2.13.1 (R Development Core Team, 2011).

5 Results

5.1 The 1982–1983 El Niño event

We first concentrate on the severe 1982–1983 El Niño episode as an example of the analyses conducted for each of the El Niño. Figure 7 shows time series plots of (a) monthly rainfall and the long-term mean, (b) (cumulative) rainfall deficit, and (c) active fire counts and ENSO index. For the 24 months surrounding this episode, a broad agreement between temporal trends in fire occurrence and drought is apparent, albeit somewhat interrupted by the November 1982–January 1983 "wet" monsoon. The ONI metric indicates that formal El Niño "warm episode" conditions commenced in May 1982, and the GAC-derived active fire data indicate that significant fire activity commenced around two months later in July 1982 (Fig. 7c), coincident with the first month of a

positive rainfall deficit (Fig. 7b). At this time, the monthly "all Borneo" mean rainfall measure fell close to the 100 mm "critical threshold" identified by Goldammer (2007), around half of the long-term mean for July, and the "Southern Borneo" precipitation became even more depressed (Fig. 7a). Such dry conditions result in the commencement of extensive leaf-shedding, surface fuel flammability increases and peatland desiccation (Brady, 1997; Goldammer, 2007), all of which are likely to have contributed to the subsequent development of many extreme fires in areas where anthropogenic ignition sources were available. Indeed, fire activity peaked two months later in September 1982, a month after the August peak in monthly rainfall deficit. Rainfall deficit remained positive until the end of ENSO Year 1, by which time fire activity had declined to low levels during the monsoon rains of November and December 1982.

Around the start of ENSO Year 2 (1983), the ENSO indices show El Niño conditions reaching peak strength (Fig. 7c). This is the time of the northeast "wet" monsoon, and in January 1983 monthly rainfall totals were actually close to the long-term mean (Fig. 7a). However, a positive rainfall deficit returned in February, followed by the highest rainfall deficits of ENSO Year 2 in March and April (Fig. 7b), coinciding with the months of peak fire activity (Fig. 7c). Rainfall returned to levels slightly higher than the long-term mean in May 1983 (Fig. 7a), with a consequent weakening of the cumulative rainfall deficit and a severe reduction in fire activity (Fig. 7c). Almost all the ENSO indices show a significant decline in El Niño strength by this time (Fig. 7c), and the ONI metric indicates that warm ENSO conditions ceased in June 1983. Unlike the other El Niño events studied here, the 1982–1983 event was not immediately followed by a La Niña (cold ENSO) episode (though of course the 1991–1992 El Niño was followed by a further set of El Niño conditions in 1993–1994, which was only then followed by La Niña). Overall, fires were much more numerous in ENSO Year 2, with the total active fire pixel count being five times higher in 1983 than in 1982 (Fig. 7c).

The AF density map for the 1982–1983 El Niño episode (Fig. 8; top left panel) indicates that fire activity was concentrated in East Kalimantan, with far less activity in West, Central and South Kalimantan. Our new satellite-derived AF data confirm previous suggestions that fires were absent from Sarawak even during this extreme El Niño event, reportedly due to the lack of severe drought in this part of Borneo (Goldammer, 2007). However, we do detect fires in Sabah, where precipitation levels apparently fell by an average of 60 % over the 1982–1983 period (Woods, 1989). In general, we see that the 1982–1983 fire activity is confined to a zone extending inland a maximum of $c.$ 200 km. Goldammer and Seibert (1990), Walsh (1995) and Goldammer (2007) report this to be the approximate area within which monthly precipitation fell below the critical 100 mm threshold, with higher rainfall generally seen within the more mountainous areas further inland (Fig. 1).

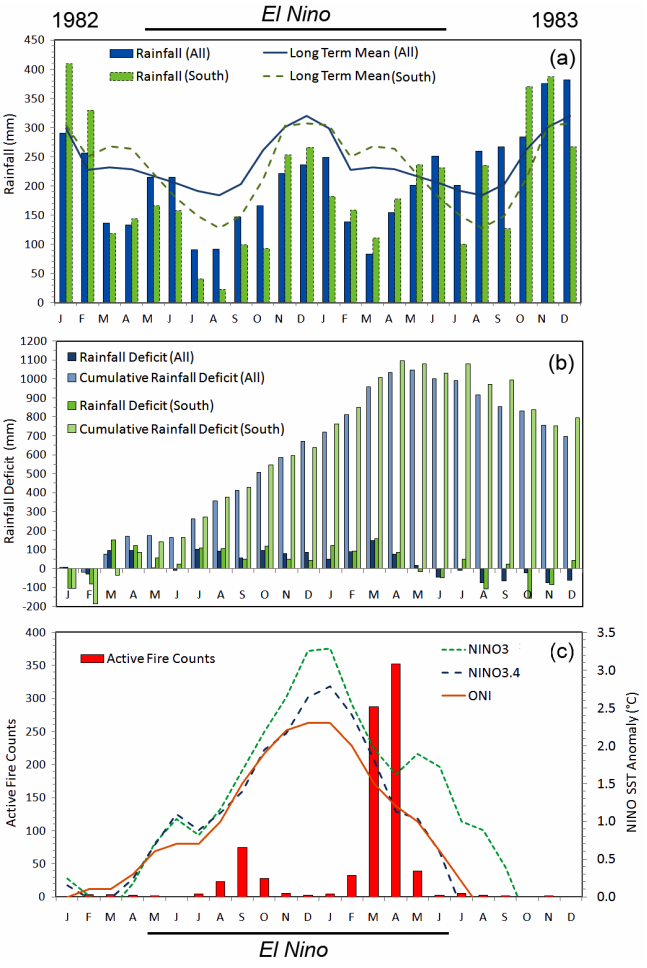

Fig. 7. Rainfall, ENSO index and active fire count data for the strong 1982–1983 El Niño. **(a)** Mean monthly rainfall for Borneo derived from the NOAA Climate Prediction Centre Merged Analysis of Precipitation dataset (Xie and Arkin, 1996, 1997), calculated for the whole of Borneo and for the south of Borneo, along with the respective long term monthly means, **(b)** rainfall deficit and cumulative rainfall deficit, calculated from the CMAP rainfall data shown in **(a)**, and **(c)** monthly active fire counts derived from 105 AVHRR GAC images, together with the matching set of NINO3, NINO3.4 and ONI SST anomaly measures taken from the NOAA Climate Prediction Centre (NOAA, 2011a). Peaks in fire activity seen in August–October 1982 and February-May 1983 broadly match the periods of greatest rainfall deficit. Months are classed as being experiencing El Niño conditions only if they have an ONI greater than or equal to 0.5 °C for a consecutive period of at least 5 months (Kousy and Higgins, 2007). The El Niño episode defined by this criterion is indicated by the black bar above and below the graphs.

5.2 Inter-El Niño patterns of fire activity

Figure 9a shows cloud and overpass adjusted active fire counts for each of the five El Niño episodes spanning the 1980–2000 period. Three "fire sub-seasons" are clearly identified; the first during August–October of ENSO Year 1, the

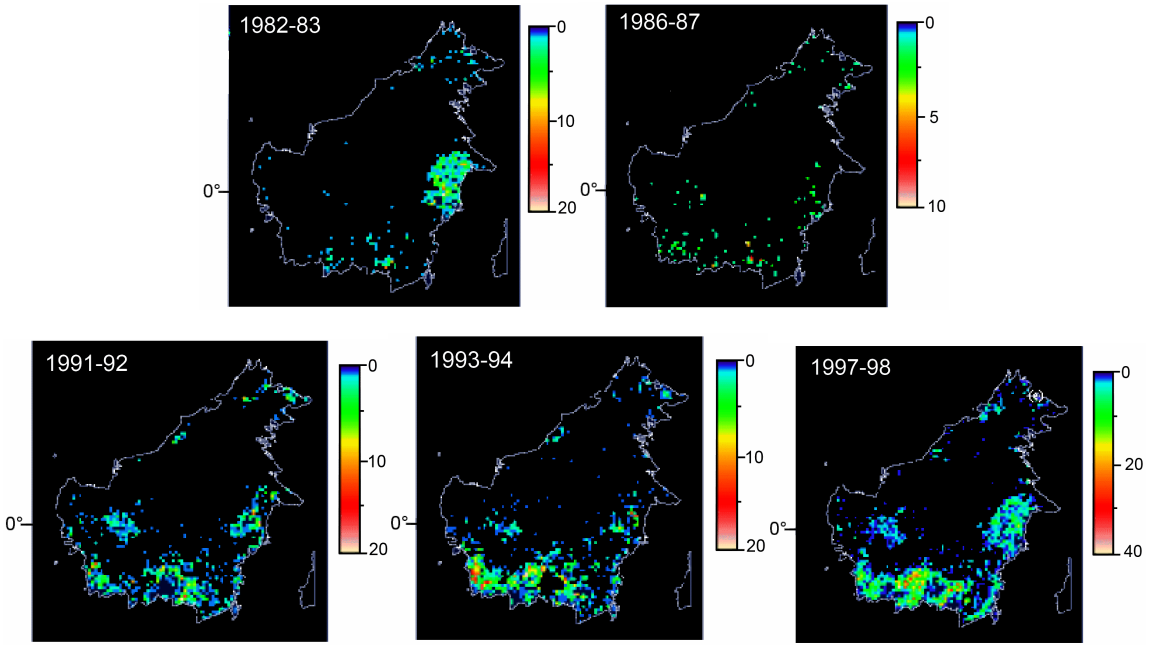

Fig. 8. Maps depicting the spatial pattern and density of active fire pixel counts detected using AVHRR GAC data during the five El Niño episodes occurring between 1980 and 2000. Grid cells are 12 km × 12 km, and colours indicate the number of active fire pixels detected in each grid cell during the full 24 months covering each El Niño event (i.e. Jan ENSO Year 1 to Dec ENSO Year 2), a period including all three fire-subseasons depicted in Fig. 9. The 1982–1983 El Niño, and to a lesser extent the 1997–1998 El Niño, are those having the highest proportion of fire activity in the northern half of the island (in East Kalimantan). Note the different colour-scales used for the 1986–1987 and 1997–1998 El Niño events, required to accommodate the relatively low and high active fire count totals seen respectively in these two El Niños.

second during February–April of ENSO Year 2, and the third during August–October of ENSO Year 2. However, only some El Niño events show fire activity during the third fire sub-season, it being absent, for example, during the major 1982–1983 El Niño. Importantly, the overall temporal pattern of fire activity shown in Fig. 9a remains the same if the fire counts remain unadjusted for cloud-cover variations, with the same rank order of fire-affected months in each El Niño year. This indicates that our results are not dependent upon assumptions made during our cloud-normalisation procedure (see Sect. 4.1.4). The ENSO index data in Fig. 9b confirm the enormity of the 1982–1983 and 1997–1998 El Niño episodes (see Table 1). Figure 9a also indicates that fire activity in these years was similarly of an overwhelming magnitude, with total AF counts respectively more than two and three times greater than those seen in the next highest event (1991–1992).

Typically, the vast majority (>80 %) of total active fire counts seen in the AVHRR-GAC record occur within the first 16-months of an El Niño event. Specifically, for the five El Niños studied here, 34 % of the total AF counts are associated with the first fire sub-season, 41 % with the second, and 18 % with the third, the latter being dominant in only the 1991–1992 and 1993–1994 El Niño's (Fig. 9a). The remaining 7 % of detected active fires occur outside of these three fire sub-seasons. By contrast, analysis of the TRMM VIRS and ERS-2 ATSR AF records indicate that in non-El Niño years the first fire sub-season accounts for the vast majority of fires (e.g. *c*. 80 % in the 1999–2000 period). The fact that the El Niño cycle often matures relatively close to the timing of the second fire sub-season (e.g. Fig. 8b) is the likely explanation for this difference, further supporting a strong link between the development of El Niño and fire.

Figure 8 illustrates the spatial pattern of fire activity for each of the additional four El Niño's studied, alongside that of the 1982–1983 event discussed in Section 5.1. These "Active Fire Density" maps confirm the relative lack of fires during the 1986–1987 El Niño episode, and the overwhelming amount of fire activity that occurred in the strongest (1997–1998) El Niño during both the first and second fire subseasons (c.f. Fig. 9a).

Later El Niños show a spatial pattern of fire rather different to that seen in 1982–1983, although fire activity remained confined to areas within *c*. 200 km of the coast. In these later El Niño episodes, fire is much more prevalent in Central and South Kalimantan, possibly due to increasing amounts of forest degradation and fragmentation (Langner and Seigert, 2009). In particular, from the 1991–1992 El Niño onwards, significant fire activity is also seen in inland parts of West Kalimantan. However, it is not until

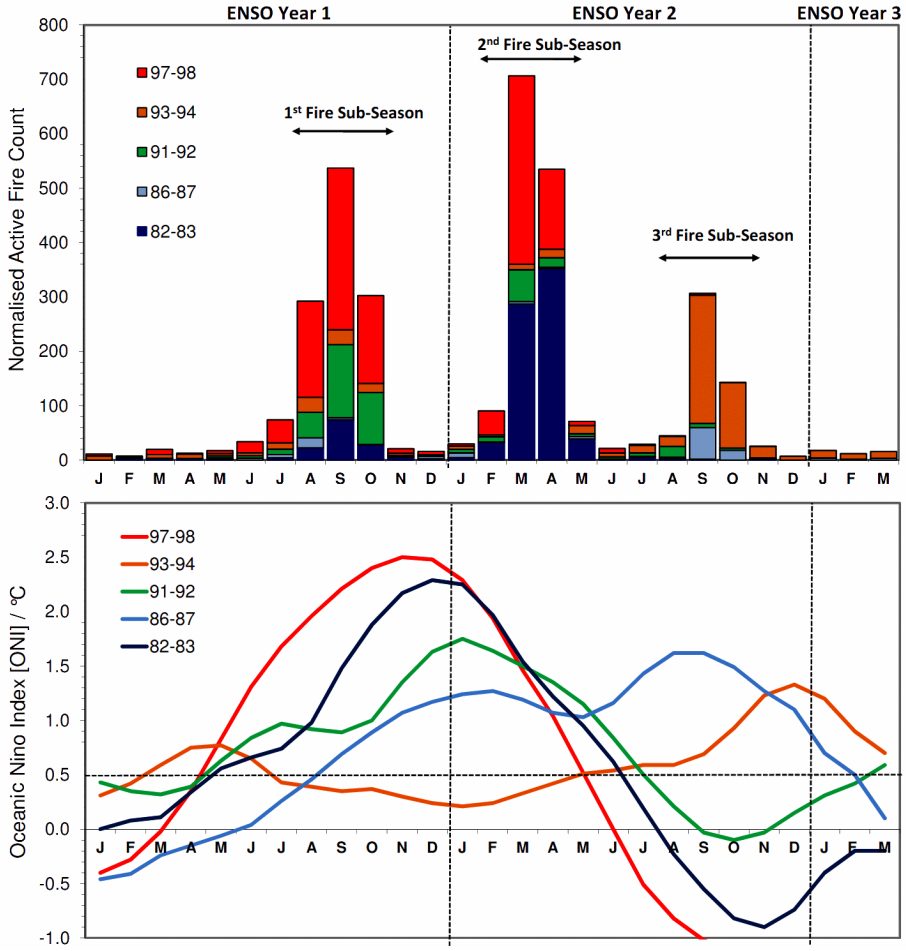

Fig. 9. Active fire and El Niño index data for the five El Niño episodes occurring between 1980 and 2000. **(a)** Monthly active fire counts derived from AVHRR GAC data, indicating the presence of three fire sub-seasons over the period of an El Niño episode. **(b)** El Niño strength as measured by the Oceanic Niño Index (ONI) measure, which is based on the three-month running mean of the NINO3.4 sea surface temperature (SST) anomaly and which is used by NOAA to classify months as showing El Niño conditions (based on an ONI threshold $\geq$0.5°C for a consecutive period of 5 months of more; Kousky and Higgins, 2007). The horizontal dashed line indicates the ONI = 0.5°C threshold. 1982–1983 and 1997–1998 are confirmed as the strongest El Niños in terms of their SST anomaly maxima, the sustained rapidly of their SST anomaly increase, and by most temporally-integrated measures of SST anomaly magnitude (°C-months; Table 1). The extreme magnitude of the 1982–1983 and 1997–1998 El Niños matches with the particularly high active fire counts recorded for these two episodes in **(a)**.

the 1997–1998 El Niño that fire activity becomes heavily concentrated in East Kalimantan once more, and this again occurs during the second fire sub-season as it did during the 1982–1983 El Niño event. Using optical remote sensing data of Borneo from 2002, Langner et al. (2007) identified areas of fire-prone "cultivation-forest mosaic" and "bare ground/grasslands/agriculture" to be primarily located along the coasts of East, South and Central Kalimantan, and in both the coastal and inland regions of West Kalimantan. The forest/non-forest maps derived in the earlier Fuller et al. (2004) study confirm this spatial distribution. Yamagata et al. (2010) recently used similar optical remote sensing data to produce a time series map of forest cover change on Borneo in the 26 yr since 1982, confirming the removal of large areas of forest in the coastal regions of East, South and Central Kalimantan, and further inland in West Kalimantan. The maps shown in Fig. 8 indicate these to be the same areas that developed by far the severest fire activity over the 1982–1998 period, helping to further confirm the strong fire-deforestation link highlighted in so many past works (e.g. Cochrane, 2003; Fuller, 2003; Goldammer, 2007; Field et al., 2009).

5.3 Relationship between El Niño, rainfall and fire

Results from our correlation analysis between ENSO strength and rainfall are reported in Table 2. They indicate ONI to be significantly correlated to monthly rainfall deficit

when considering all months of all five El Niños together (i.e. the first row of Table 2) for the whole of Borneo (ABD; $r = 0.48$), and also when only considering rainfall in the southernmost part of the island only (SBD; $r = 0.35$). Correlations using the NINO3 and NINO3.4 metrics are weaker (Table 2).

On a per-El Niño basis, monthly rainfall deficit is much more strongly correlated with El Niño intensity (in particular as measured via the ONI index) during the strongest 1982–1983 and 1997–1998 events (Table 2), than during the intervening (and weaker) El Niños (1986–1987, 1991–1992 and 1993–1994). Aldrian and Susanto (2003) report that whilst the rainfall regime of south and Central Kalimantan appears to be significantly impacted by El Niño, that in Eastern Kalimantan it is less so. This may in part explain why large numbers of fires are only seen in East Kalimantan during the two most intense El Niños (Fig. 8). Results for NINO3 and NINO3.4 are qualitatively similar to those obtained using ONI, and correlations between El Niño strength and rainfall are also generally stronger when considering the whole of Borneo than just the southernmost part of the island, and when considering all months of each El Niño episode rather than just those months meeting the ONI $\geq$0.5 °C criteria.

Table 3 reports the results of the cross-correlation analysis between active fire count and rainfall deficit, separated into four subsets (those based on all months and just those meeting the ONI $\geq$0.5 °C criteria, and those using rainfall deficit data for all Borneo (ABD) and just Southern Borneo "SBD"). The results reveal a robust relationship, and when analysing the same variables the correlation coefficient (r) for most of the El Niños is of a similar strength. In the case of the 1986–1987, 1991–1992 and 1993–1994 El Niño's, the correlations are generally (but not consistently) slightly stronger for the Southern Borneo than for the all Borneo rainfall deficit data set. The reverse is true for the 1982–1983 and 1997–1998 El Niño's, perhaps because these two events have the greatest proportion of their fire activity north of the Equator (i.e. in East Kalimantan, see Fig. 8). The correlation between active fire count and rainfall deficit peaks at zero lag (i.e. simultaneously) or one-month lag for all five El Niños (r values between 0.4 and 0.5), except for the 1986–1987 event (where it peaks at -9 months, although this association is not statistically significant). This (near) simultaneous rainfall-fire association is generally somewhat stronger for the post-1990 El Niño events than for earlier El Niño's; and indeed, the relationship between rainfall deficit and fire activity is shown to have been relatively weak in 1982–1983 (albeit less so in the all months/all-Borneo data subset). Again, this possibly reflects the increased amounts of forest degradation that apparently occurred during the 1990s (FWI/GFW, 2002), and the fact that degraded forest and agricultural areas are likely to respond more rapidly to precipitation deficits than are closed canopy wet forests, which can maintain fuel moisture levels for some weeks even during drought (Guhardja et al., 2000; Cochrane, 2003).

A similar cross-correlation analysis was applied to the monthly active fire (AF) pixel count and ENSO index (ONI, NINO3, NINO3.4) data , based on both all months in an El Niño episode, and just months with ONI $\geq$0.5 °C (Table 4). Of the three indices tested, the strongest relationship between AF counts and El Niño strength was found using the ONI index, where r lay in the range 0.29–0.63; for the NINO3 and NINO3.4 indices r was typically around 0.30–0.40. For the 1982–1983, 1986–1987 and 1997–1998 El Niños, correlations between AF and ENSO index tended to be stronger than for AF and rainfall deficit, but it was found to be weaker for the 1991–1992 and 1993–1993 events. The relationship between peak ENSO index and peak fire occurrence timing varied between El Niño episodes and El Niño metrics; the ONI index showed the strongest correlation at zero-lag for all except the 1982–1983 event where the cross-correlation strength peaked at a lag of three months (Table 4). The NINO3 and NINO3.4 indices typically peaked at lags of between three and fourth months, but lag peaks varied between zero and nine months for different El Niño events. This possibly reflects the teleconnection lag between El Niño and Indonesian climate variables, and the time over which different forest and non-forest fuels, and regions of Borneo subject to different levels of forest degradation and clearance, become increasingly flammable during drought. The differing lag times may also be related to variations in the timing of the El Niño-related sea surface temperature anomaly development in the various regions of the Pacific Ocean used to calculate the ENSO indices (Fig. 1c), and the action of the monsoon rains, which outweigh the precipitation-reducing influence of El Niño during the monsoon periods.

We complemented our time series analysis with a comparison of time-integrated AF count and El Niño strength, with the latter measured via cumulative NINO-X anomalies. Three integration times were considered for each El Niño event studied here, (1) the 16 months from the start of ENSO Year 1 to the end of the 2nd fire sub-season in ENSO Year 2, (2) the full ENSO Year 1 and ENSO Year 2 period, and (3) only months showing ONI$\geq$05 °C. Results, reported in Table 5, indicate that the strongest positive statistical relationship ($r = 0.98$) was found using the NINO3 index over the first and second fire sub-seasons only (i.e. January ENSO Year 1 to April ENSO Year 2). This relationship, shown in Fig. 10, of course omits fires occurring in the third fire subseason (August–October of ENSO Year 2). Relationships using the NINO3.4 and ONI indices were also strongly positive over this same 16 month period (Table 5, cols 1–3). Excluding the 1993–1994 El Niño, which showed the highest proportion of third fire sub-season activity (Fig. 9a), a strong linear relationship ($r = 0.90$) with the cumulative NINO3 index is also seen when extending the cumulative fire count record included in Fig. 10 to the entire 24 months (i.e. Jan ENSO Year 1 to Dec ENSO Year 2) of each El Niño episode. The 1993–1994 El Niño is unusual in that it immediately followed the 1991–1992 El Niño (Trenberth and Hoar, 2006),

Table 2. Correlation (r) between monthly El Niño strength (as measured by the ONI, NINO3, and NINO3.4 SST anomaly-based indices) and Borneo's rainfall deficit across the whole island (ABD) and just the south of the island (SBD) during the five El Niños studied here; the two most significant in terms of El Niño strength being those of 1982–1983 and 1997–1998. Results are shown for individual events and all events pooled together, and including all months (total = 126 across all years) and only those months meeting only the ONI≥0.5 °C criteria (Kousky and Higgins, 2007).

All months							
		ONI		NINO3 Anomaly		NINO3.4 Anomaly	
Year	n	ABD	SBD	ABD	SBD	ABD	SBD
Pooled	126	0.48	0.35	0.28	0.15	0.38	0.28
1982–1983	24	0.72	0.57	0.60	0.52	0.69	0.60
1986–1987	27	0.30	0.18	0.03	−0.32	0.25	0.05
1991–1992	24	0.37	0.11	0.21	0.08	0.20	0.02
1993–1994	27	0.060	−0.11	−0.49	−0.63	−0.28	−0.34
1997–1998	24	0.67	0.55	0.59	0.46	0.63	0.52
Months with ONI>0.5 °C							
		ONI		NINO3 Anomaly		NINO3.4 Anomaly	
Year	n	ABD	SBD	ABD	SBD	ABD	SBD
Pooled	76	0.46	0.32	0.14	−0.01	0.24	0.15
1982–1983	14	0.51	0.37	−0.04	−0.05	0.16	0.17
1986–1987	19	0.22	0.30	−0.04	−0.21	0.01	0.07
1991–1992	15	0.19	−0.21	−0.09	−0.39	−0.15	−0.50
1993–1994	15	0.09	−0.14	−0.56	−0.68	−0.34	−0.48
1997–1998	13	0.64	0.50	0.04	−0.35	0.48	0.37

Table 3. Correlation (r) between monthly rainfall deficit (across all Borneo [ABD] and Southern Borneo [SBD]) and fire activity (active fire counts) during the five El Niño events studied here; the two most significant in terms of El Niño strength being those of 1982–1983 and 1997–1998. The upper table shows analyses based on all months during an El Niño episode, the lower table only those months having ONI>0.5 °C (note: in 1993–1994 there were multiple periods with ONI>0.5 °C and so only the entire episode was analysed). Zero-lag is the strength of association at lag = 0 months; Max r is the lag (in months) showing the strongest correlation, and Strong lag is the strength of the correlation in that month.

All months						
	ABD			SBD		
Year	Zero-lag	Max r	Strong lag	Zero-lag	Max r	Strong lag
1982–1983	0.41	−1	0.47	0.33	−1	0.40
1986–1987	0.27	−9	0.37	0.35	0	0.35
1991–1992	0.48	0	0.48	0.50	0	0.50
1993–1994	0.41	0	0.41	0.48	0	0.48
1997–1998	0.47	0	0.47	0.44	0	0.44
ONI>0.5 °C						
	ABD			SBD		
Year	Zero-lag	Max r	Strong lag	Zero-lag	Max r	Strong lag
1982–1983	0.37	−1	0.44	0.28	−1	0.34
1986–1987	0.23	−9	0.43	0.37	0	0.37
1991–1992	0.48	0	0.48	0.50	0	0.50
1993–1994						
1997–1998	0.46	0	0.46	0.42	0	0.42

Table 4. Correlation (r) between monthly El Niño strength (as measured by the ONI, NINO 3, and NINO 3.4 ENSO index anomalies) and fire activity (AF counts) during the five El Niño events studied here; the two most significant in terms of El Niño strength being those of 1982–1983 and 1997–1998. The upper table shows analyses based on all months during the episode, the lower only those where the ONI>0.5 °C (note in 1993–1994 there were multiple periods with ONI>0.5 °C and so only the entire episode was analysed). Zero-lag is the strength of association at lag = 0; Max r is the lag with the strongest positive correlation and Strong lag the strength of the correlation in that month.

All months									
		ONI			NINO3 Anomaly			NINO3.4 Anomaly	
Year	Zero-lag	Max r	Strong lag	Zero-lag	Max r	Strong lag	Zero-lag	Max r	Strong lag
1982–1983	0.38	−3	0.59	0.46	0	0.46	0.35	−3	0.36
1986–1987	0.51	0	0.51	−0.08	−5	0.42	0.19	−3	0.34
1991–1992	0.32	0	0.32	−0.15	−4	0.24	−0.02	−3	0.27
1993–1994	0.29	0	0.29	−0.35	−5	0.31	−0.14	−4	0.36
1997–1998	0.63	0	0.63			0.44	0.43	0	0.43
ONI>0.5 °C									
		ONI			NINO3.4 Anomaly			NINO3.4 Anomaly	
Year	Zero-lag	Max r	Strong lag	Zero-lag	Max r	Strong lag	Zero-lag	Max r	Strong lag
1982–1983	0.20	−3	0.69	0.47	0	0.47	0.28	−3	0.53
1986–1987	0.41	0	0.41	−0.13	−5	0.48	0.06	−3	0.34
1991–1992	0.16	0	0.16	−0.42	−4	0.21	−0.29	−9	0.20
1993–1994									
1997–1998	0.43	0	0.43	0.27	−3	0.30	0.24	−3	0.34

and was characterised by NINO3, NINO3.4 and ONI indices that peaked early in ENSO Year 1, weakened significantly over the following 12 months, and then peaked again in the third fire sub-season (Fig. 9b). The unusual nature of this El Niño event probably explains the occurrence of so much fire activity in the 1993–1994 third fire sub-season (as seen in Fig. 9a). With all El Niño events considered, and all three fire sub-seasons (i.e. a two year integration period), the strongest linear relationship ($r = -0.98$) was actually found using the cumulative NINO4 index, with a strong inverse correlation when considered over the full ENSO Year 1 and Year 2 period (Table 5, cols 5–7). The negative relationship between time-integrated fire activity and the NINO4 index reflects the fact that the 24 month cumulative SST anomaly measured in the NINO4 region (western tropical pacific; Fig. 1c) is itself negatively correlated ($r = -0.83$) with that in NINO3 (Eastern Tropical Pacific; Fig. 1c). Therefore, the greater the cumulative NINO3 SST anomaly the weaker that seen in NINO4, reflecting the different sea surface temperature patterns seen during ENSO events across the tropical Pacific. For example, in Fig. 1c it is apparent that around the time of maximum positive NINO3 and NINO3.4 anomalies seen during the extreme 1997–1998 El Niño (December 1997), significant parts of the NINO4 region are already showing negative SST anomalies associated with cooler than normal surface waters. The underlying drivers of these relationships may also be influenced by the fact that the strongest El Niño events studied here (1982–1983 and 1997–1998) have been classed as "cold tongue" El Niños (characterised by large positive SST anomalies in the NINO3 region), whereas the remaining events are classed as "warm pool" El Niños (whose effect on SST is considered more confined to the NINO4 region) (Kug et al., 2009). Table 5 also indicates that linear relationships between cumulative fire count and cumulative ENSO indices derived using only data from months with an ONI>0.5 °C are weaker than those derived using all months of data, reflecting the potential for significant lags between the developing strength of El Niño and fire activity (Sect. 5.3).

6 Disscusions and conclusions

Large parts of Borneo have been subject to (still ongoing) land clearance, peatland draining and general forest degradation activities over many decades, resulting in a landscape where huge areas of the natural ecosystem have been replaced by degraded, converted, or managed cover types, with many anthropic ignition events and vegetation fires. When such changes are accompanied by extreme drought, which in Borneo are usually associated El Niño (i.e. warm ENSO) conditions, areas of normally moist peatland and forest can much more easily dry, ignite and burn than would otherwise be the case. These conditions enable the anthropically driven fires to further spread and intensify, resulting in fire events

Table 5. Correlation (r) between time-integrated El Niño strength (as measured by the ONI, NINO3, NINO4, NINO3.4 ENSO index anomalies) and fire activity (AF counts) integrated over the same time period. Results are shown for the five consecutive El Niño events studied here (1982–1983 to 1997–1998); the two most significant in terms of El Niño strength being those of 1982–1983 and 1997–1998. Three integration periods are tested (1) the 16 months from the start of ENSO Year 1 to the end of the 2nd fire sub-season in April ENSO Year 2, (2) the full 24 months of ENSO Year 1 and ENSO Year 2, and (3) the months showing ONI≥05 °C for each ENSO event (this metric covers different numbers of months in each ENSO episode) as detailed in Table 1.

	Jan Yr1 1 – Apr Yr 2 (16 months)			Jan Yr 1 – Dec Yr 2 (24 months)			Months with ONI≥05 °C		
Year	r	slope	intercept	r	slope	intercept	r	slope	intercept
NINO3	0.98	43.1	−69.3	0.69	31.7	148.1	0.66	24.7	181.0
NINO3.4	0.93	59.3	−259.4	−0.14	−18.69	954.7	0.37	21.7	257.3
ONI	0.93	72.1	−479.3	−0.42	−81.59	2041.7	0.41	45.0	−192.2
NINO4	0.53	97.9	−199.1	−0.98	−91.0	1442.7	−0.58	−77.1	1306.6

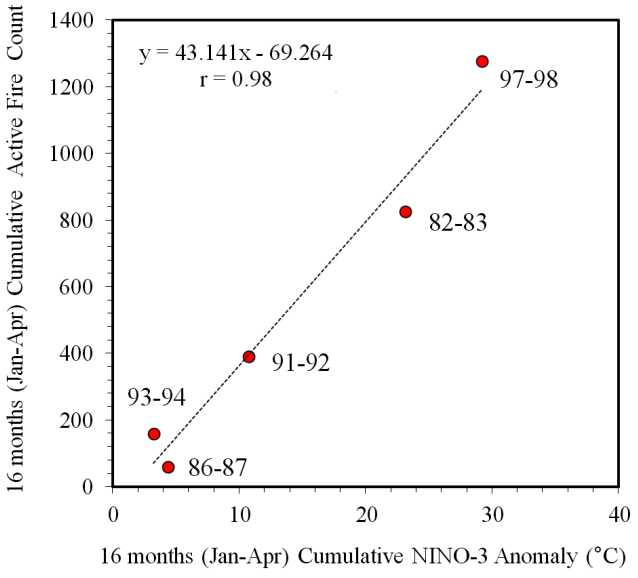

Fig. 10. Relationship between Borneo's cumulative active fire count derived from AVHRR GAC imagery (calculated from the monthly data shown in Fig. 9) and cumulative El Niño strength, here calculated from the integration of the NINO3 anomaly index over the 16 months of each El Niño encompassing the first and second fire sub-seasons defined in Sect. 5.2 (i.e. Jan ENSO Year 1 to Apr ENSO Year 2). The linear best fit to the data is shown, and the alternative relationships calculated for other durations and using alternative ENSO indices are shown in Table 5.

that can be of an extreme magnitude and which can have significant impacts on forest, flora and fauna (Goldammer, 2007; Barlow and Silveira, 2009), fossil peatland stores (Page et al., 2009), and global greenhouse gas concentrations (Page et al., 2002; Simmonds et al., 2005). They also result in major regional haze episodes with significant health implications for the health of many tens of millions of humans, including outside Indonesia (Aditama, 2000; Emmanuel, 2000; Kunii et al., 2002; Aiken, 2004; Heil et al.,2007; Naeher et al., 2007).

This work is the first to comprehensively analyse and intercompare active fire (AF) signals present in terrestrial remote sensing data of Borneo for the five El Niño events that occurred between 1982 and 1998, immediately prior to operation of the current MODIS Earth Observation sensor that is widely used for active fire studies. We have used AVHRR Global Area Coverage (GAC) data to detect and quantify the relative number of fires burning across Borneo in each month of each El Niño event, and our work complements previous studies that used atmospheric data to quantify variations in biomass burning occurring over similar time periods (e.g. Kita et al., 2000; Duncan et al., 2003; Field et al., 2009). The 20 yr period we have examined includes the extreme 1982–1983 and 1997–1998 El Niños, which by all common measures are the strongest since 1950 and quite possibly since 1877–1978 (Wolter and Timin, 1998). Our results reveal that during the two strongest El Niños, there is a relatively strong correlation between monthly measures of El Niño strength (specifically the Operational Niño Index [ONI]; Kousky and Higgins, 2007) and monthly rainfall deficit ($r = 0.715$ and $r = 0.673$ respectively). These two strongest El Niños also show two clearly distinguishable fire sub-seasons, and a consistent correlation between the El Niño-driven rainfall deficit and the number of active fire counts that peaks at 0 or 1 month lag. The vast majority of fire activity in these events occurs during August–October of ENSO Year 1 (first fire sub-season) and February–April of ENSO Year 2 (second fire sub-season). In the intermediate period (November–January) monsoon rains temporarily weaken El Niño's influence by breaking the associated drought, resulting in an almost complete absence of fire. During some of the other El Niño episodes (most particularly that of 1993–1994), major fires also occur during a third fire sub-season (August–October of ENSO Year 2), but total fire numbers are fewer and the correlation between El Niño strength and monthly rainfall deficit is less strong for these weaker El Niño's.

We also find that the correlation between monthly El Niño strength and fire activity is for some El Niños stronger than between rainfall deficit (drought) and fire. The magnitude of fire activity appears to be related both to the duration of El Niño conditions, as well as to its strength. For example, the unprecedented duration of the 1991–1994 El Niño (here separated into 1991–1992 and 1993–1994) resulted in severe fires, despite peak ENSO index values being similar to 1986–1987, when fire activity was much lower. Fuller and Murphy (2006) previously found a weakly significant three month lag between the Southern Oscillation Index (SOI; based on atmospheric pressure differences between Darwin and Tahiti) and fire activity during the 1996–2001 period, whereas we found the strongest relationship between El Niño strength (as described by the ONI) and AF counts occurred at zero-lag for all except the 1982–1983 El Niño event. For this latter event, the cross-correlation peaked at a lag of three months, while other ENSO indices showed typical peak lag times of three to four months, but varied up to nine months, across the five El Niño's studied. Among the various ENSO indices tested, the time-integrated (i.e. cumulative strength) NINO3 anomaly showed the strongest positive linear relationship with the total number of active fire counts measured over the 16 months covering the first and second fire sub seasons, explaining 97 % of the variation seen over the five El Niño's examined. In a similar vein, Fuller and Murphy (2006) found that annual sums of the southern oscillation index (SOI) are strongly associated with variations in annual fire activity in Borneo under conditions when the annual SOI sum is negative. Including in addition the third fire sub-season, the cumulative NINO4 anomaly showed an equally strong but negative linear relationship with the cumulative active fire count ($r = -0.98$).

Relationships between El Niño strength, drought, and fire activity potentially provide the basis for an empirical ENSO index-based fire-forecasting scheme for Borneo; and such a tool could be used to help predict and perhaps mitigate the fire-related impacts of future El Niño's (see also Fuller and Murphy, 2006). Seasonal forecasting of ENSO indices is now quite routine and capable of delivering reasonable levels of skill many months in advance (e.g. Chen et al., 2004; Jin et al., 2008), and such forecasts could be used alongside the El Niño-fire relationships established here to evaluate the potential magnitude of forthcoming fire activity and to assess the likelihood of major ecological, atmospheric and human health impacts. However, our study of links between El Niño and fire is underpinned by only five El Niño events, and we assume a stationary relationship. This may not be the case for a dynamically unstable process such as a fire regime, and future changes in land cover, vegetation composition and structure, etc. may alter El Niño-fire relations (e.g. via the types of positive feedback loops described by e.g. Cochrane, 2003). Much higher sample numbers (50 yr or more) have typically been used to develop robust El Niño-fire relationships in the Americas (e.g. Simard et al., 1985; Swetnam and Betancourt, 1990; Kitzberger, 2002), although recent work in the Amazon has indicated that robust relationships maybe possible even with the limited time series of data now available from active fire remote sensing from space (Chen et al., 2011) and that we have begun to demonstrate here for Southeast Asia.

Acknowledgements. We are grateful for the station rainfall data for the Indonesian part of Borneo provided to us by Dewi Kirono and Nigel Tapper (Monash University, Australia) and collected originally by the Indonesian Bureau of Meteorology and Geophysics (Badan Meteorologi dan Geofisika, BMG). In addition, monthly rainfall data from four additional stations for the 1980–1998 period was accessed for Sabah and Sarawak, the Malaysian part of Borneo, via the NOAA Climate Prediction Centre (USA) and the UK Meteorological Office. CMAP Precipitation data were provided by the NOAA/OAR/ESRL PSD, Boulder, Colorado, USA, from their Web site at http://www.esrl.noaa.gov/psd/, while TRMM precipitation data were provided by the NASA Global Change Master Directory (www.gcmd.nasa.gov). We are also extremely grateful to Louis Giglio (University of Maryland) for the TRMM-derived information depicting the diurnal fire cycle of Borneo. Remote Sensing Systems (www.remss.com) are thanked for the SST anomaly maps. Funding for this study was contributed to by the NERC QUEST programme (NE/F001584/1) and A. Zoumas was supported by the State Scholarships Foundation (IKY) of Greece. We thank Guido van der Werf and Andreas Langer for their useful reviews, and in particular Angelika Heil for her detail, care and attention in suggesting improvements to our manuscript.

Edited by: A. Arneth

References

Aditama, T. Y.:Impact of haze from forest fire to respiratory health: Indonesian experience, 5, 169–174, 2000.

Aiken, R.: Runaway fires, smoke-haze pollution and unnatural disasters in Indonesia, Geogr. Rev., 994, 55–79, doi:10.1111/j.1931-0846.2004.tb00158.x, 2004.

Aldrian, E. and Susanto, R. D.: Identification of three dominant rainfall regions within Indonesia and their relationship to sea surface temperature, Int. J. Climatol., 23, 1435–1452, 2003.

Aldrian, E., Gates, L. D., and Widodo, F. H.: Seasonal variability of Indonesian rainfall in ECHAM4 simulations and in the reanalyses: The role of ENSO, Theor. Appl. Climatol., 87, 41–59, 2007.

Alencar, A., Nepstad, D., and Diaz, M. D. V.: Forest understory fire in the Brazilian Amazon in ENSO and non-ENSO years: area burned and committed carbon emissions, Earth Interact., 10, 1–17, doi:10.1175/EI150.1, 2006.

Baker, P. J. and Bunyavejchewin, S.: Fire behaviour and fire effects across the forest landscape of continental Southeast Asia, in: Tropical Fire Ecology, edited by: Cochrane, M. A., 311–334, Springer Berlin Heidelberg, 2009.

Barnston, A. G., Li, S., Mason, S. J., DeWitt, D. G., Goddard, L., and Gong, X.: Verification of the First 11 Years of IRI's Seasonal Climate Forecasts. J. Appl. Meteorol. Clim., 49, 493–520, 2010.

Barlow, J. and Silveira, J. M.: The consequences of fire for the fauna of humid tropical forests, in: Tropical Tire Ecology, edited by: Cochrane, M., Springer Praxis Books, 543–556, 2009.

Brady, M.: Organic matter dynamics of coastal peat deposits in Sumatra, Indonesia, Doctoral dissertation, University of British Columbia, 1997.

Chatfield, C.: The Analysis of Time Series: An Introduction, Chapman and Hall, CRC., Boca Raton, Florida, 2004.

Chen, D., Cane, M. A., Kaplan, A., Zebiak, S. E., and Daji, H.: Predictability of El Niño over the past 148 years, Nature, 428, 733–736, 2004.

Chen, Y., Randerson, J. T., Morton, D. C., DeFries, R. S., Collatz, G. J., Kasibhatla, P. S., Giglio, L., Jin, Y., and Malier, M. E.: Forecasting fire season severity in South America using sea surface temperature anomalies, Science, 334, 787–791, 2011.

Chuvieco, E., Giglio, L., and Justice, C.: Global characterization of fire activity: toward defining fire regimes from Earth observation data, Glob. Change Biol., 14, 1–15, doi:10.1111/j.1365-2486.2008.01585.x, 2008.

Cochrane, M.: Fire science for rainforests, Nature, 421, 913–919, doi:10.1038/nature01437, 2003.

Couwenber, J., Dommain, R., and Joosten, H.: Greenhouse gas fluxes from tropical peatlands in Southeast Asia, Glob. Change Biol., 16, 1715–1732, doi:10.1111/j.1365-2486.2009.02016.x, 2010.

Curran, L. M., Trigg, S. N., McDonald, A. K., Astiani, D., Hardiono, Y. M.,; Siregar, P., Caniago, I., and Kasischke, E.: Lowland Forest Loss in Protected Areas of Indonesian Borneo, Science, 303, 1000–1003, doi:10.1126/science.1091714, 2004.

Duncan, B. N., Martin, R. V., Staudt, A. C., Yevich, R., and Logan, J. A.: Interannual and seasonal variability of biomass burning emissions constrained by satellite observations, J. Geophys. Res., 108, 4100, doi:10.1029/2002JD002378, 2003.

Deeming, J. E.: Development of a fire danger rating system for East-Kalimantan, IFFM short term report, Document No. 08, Final report, GTZ, Eschborn, 1995.

Dennis, R.: A review of fire projects in Indonesia, 1982–1998, Center for International Forestry Research, SMT Grafika Desa Putera, Jakarta, 106pp., 1999.

Edwards, P. G., Berutti, B., Blythe, P., Callies, J., Carlier, S., Fransen, C., Krutsch, R., Lefebvre, A-R., Loiselet, M., and Stricker, N.: The MetOp satellite – Weather information from polar orbit, ESA Bull., 127, 8–17, 2006.

Emmanuel, S. C.: Impact to lung health of haze from forest fires: the Singapore experience, Respirology, 5, 175–182, 2000.

Fernandes, K., Baethgen, W., Bernardes, S., DeFries, R., DeWitt, D., Goddard, L., Lavado, W., Lee, D., Padoch, C., Pinedo-Vasquez, M., and Uriarte, M.: North Tropical Atlantic influence on Western Amazon fire season variability, Geophys. Res. Lett., 38, L12701, doi:10.1029/2011GL047392, 2011.

Field, R. D., van der Werf, G. R., and Shen, S. S. P.: Human amplification of drought-induced biomass burning in Indonesia since 1960, Nature Geosci., 2, 185–188, 2009.

Fuller, D., Jessup, T. C., and Salim, A.: Loss of forest cover in Kalimantan, Indonesia since the 1997–1998 El Niño, Conserv. Biol., 18, 249–254, 2004.

Fuller, D.: MODIS data used to study 2002 fires in Kalimantan, Indonesia, EOS Transactions of AGU, 84, 20, 189–192, 2006.

Fuller, D. O. and Fulk, M.: Comparison of NOAA-AVHRR and DMSP-OLS for operational fire monitoring in Kalimantan, Indonesia, Int. J. Remote Sens., 21, 181–187, 2000.

Fuller, D. O. and Murphy, K.: The ENSO-fire dynamic in insular Southeast Asia, Climatic Change, 74, 435–455, 2006.

FWI/GFW: The state of the forest: Indonesia, Bogor: Forest Watch Indonesia and Global Forest Watch, Indonesia and Washington DC, 85pp, 2002.

Giglio, L.: Characterization of the tropical diurnal fire cycle using VIRS and MODIS observations, Remote Sens. Environ., 108, 407–421, doi:10.1016/j.rse.2006.11.018, 2007.

Giglio, L., Descloitres, J., Justice, C. O., and, Kaufman, Y.: An enhanced contextual fire detection algorithm for MODIS, Remote Sens. Environ., 87, 273–282, 2003a.

Giglio, L., Kendall, J. D., and Mack, R.: A multi-year active fire dataset for the tropics derived from the TRMM VIRS, Int. J. Remote Sens., 24, 4505–4525, 2003b.

Giglio, L., Csiszar, I., and Justice, C. O.: Global distribution and seasonality of active fires as observed with the Terra and Aqua Moderate Resolution Imaging Spectroradiometer (MODIS) sensors, J. Geophys. Res., 111, G02016, doi:10.1029/2005JG000142, 2006.

Goldammer, J.: History of equatorial vegetation fires and fire research in Southeast Asia before the 1997–1998 episode: a reconstruction of creeping environmental changes, Mitigation and Adaptation Strategies for Global Change, 12, 13–32, 2007.

Goldammer, J. G. and Seibert, B.: The impact of droughts and forest fires on tropical lowland rainforest of Eastern Borneo, in: Fire in the Tropical Biota: Ecosystem Processes and Global Challenges, edited by: Goldammer, J. G., Ecological Studies, Springer-Verlag, Berlin, Heidelberg and New York, 84, 11–31, 1990.

Guhardja, E., Fatawi, M., Sutisna, M., Mori, T., and Ohta, S.: Rainforest Ecosystems of East Kalimantan, El Niño, Drought, Fire and Human Impacts, Ecological Studies, Springer, New York, 140, 331pp, 2000.

Gutman, G., Csiszar, I., and Romanov, P.: Using NOAA/AVHRR products to monitor El Niño impacts: focus on Indonesia in 1997–1998., B. Am. Meteorol. Soc., 81, 1189–1205, 2000.

Hamada, J.-I., Yamanaka, M. D., Matsumoto, J., Fukao, S., Winarso, P. A., and Sribi-mawati, T.: Spatial and temporal variations of the rainy season over Indonesia and their link to ENSO, J. Meteorol. Soc. Jpn., 80, 285–310, 2002.

Haylock, M. and McBride, J. L.: Spatial coherence and predictability of Indonesian wet season rainfall., J. Climate, 14, 3882–3887, 2001.

Heald, C. L., Jacob, D. J., Palmer, P. I., Evans, M. J., Sachse, G. W., Singh, H. B., and Blake, D. R.: Biomass burning emission inventory with daily resolution: Application to aircraft observations of Asian outflow, J. Geophys. Res., 108, 8811, doi:10.1029/2002JD003082, 2003.

Heil, A., Langmann, B., and Aldrian, E.: Indonesian peat and vegetation fire emissions: Study on factors influencing large-scale smoke haze pollution using a regional atmospheric chemistry model, Mitigation and Adaptation Strategies for Global Change, 12, 113–133, doi:10.1007/s11027-006-9045-6, 2007.

Holz, A. and Veblen, T. T.: Variability in the Southern Annular Mode determines wildfire activity in Patagonia, Geophys. Res. Lett., 38, L14710, doi:10.1029/2011GL047674, 2011.

Huffman, G. J., Adler, R. F., Arkin, P., Chang, A., Ferraro, R., Gru-

ber, A., Janowiak, J., McNab, A., Rudolph, B., and Schneider, U.: The Global Precipitation Climatology Project (GPCP) Combined Precipitation Dataset, B. Am. Meteorol. Soc., 78, 5–20, 1997.

Ickoku, C., Giglio, L., Wooster, M. J., and Remner, L. A.: Global characterization of biomass-burning patterns using satellite measurements of fire radiative energy, Remote Sens. Environ., 112, 2950–2962, 2008.

Jaenicke, J., Rieley, J. O., Mott, C., Kimman, P., and Siegert, F.: Determination of the amount of carbon stored in Indonesian peatlands, Geoderma, 147, 151–158, 2008.

Jin, E. K., Kinter III, J. L., Wang, B., Park, C.-K., Kang, L.-S., Kirtman, B. P., Kug, J.-S., Kumar, A., Luo, J.-J., Schemm, J., Shukla, J., and Yamagata, T.: Current status of ENSO prediction skill in coupled ocean-atmosphere models, Clim. Dynam., 31, 647–664, 2008.

Jones, C. D. and Cox, P. M.: On the significance of atmospheric CO_2 growth rate anomalies in 2002–2003, Geophys. Res. Lett., 32, L14816, doi:10.1029/2005GL023027, 2005.

Kaufman, Y. J., Setzer, A., Justice, C., Tucker, C. J., and Fung, I.: Remote sensing of biomass burning in the tropics, in: Fires in the Tropical Biota, edited by: Goldammer, J. G., Ecosystem Processes and Global Challenges, 371–399, 1990.

Kirono, D. G. C.: Principal component analysis for identifying period of seasons in Indonesia, Indonesian J. Geogr., 36, 109–121, 2004.

Kirono, D. G. C., Tapper, N. J., and McBride, J. L.: Documenting Indonesian rainfall in the 1997/1998 El Niño event, Phys. Geogr., 20, 422–435, 1999.

Kita, K., Fujiwara, M., and Kawakami, S.: Total ozone increase associated with forest fires over the Indonesian region and its relation to the El Niño-Southern oscillation, Atmos. Environ., 34, 2681–2690, 2000.

Kitzberger, T.: ENSO as a forewarning tool of regional fire occurrence in Northern Patagonia, Argentina, Int. J. Wildland Fire, 11, 33–39, 2002.

Koffi, B., Grégoire, J.-M., and Eva, H. D.: Satellite monitoring of vegetation fires on a multiannual basis at continental scale in Africa, in: Modelling and Inventory Development, and Biomass Burning in Africa, Biomass Burning and Global Change, Vol. 1, Remote Sensing, edited by: Levine, J. S., The MIT Press, Cambridge, London, 225–235, 1996.

Kousky, V. E. and Higgins, R. W.: An Alert Classification System for monitoring and assessing the ENSO Cycle, Weather Forecasting, 22, 353–371, doi:10.1175/WAF987.1, 2007.

Kug, J.-S., Fei-Fei, J., and Soon-Il, A.: Two Types of El Niño Events: Cold Tongue El Niño and Warm Pool El Niño, J. Climate, 22, 1499–1515, 2009.

Kunii, O., Kanagawa, S., Yajima, I., Yoshiharu, H., and Sombo-Yamamura, T.: The 1997 Haze Disaster in Indonesia: Its Air Quality and Health Effects, Arch. Environ. Health: An International Journal, 57, 16–22, 2002.

Langaas, S.: Senegalese fire activity during the 1989–1990 dry season deduced from NOAA AVHRR night time images, Int. J. Remote Sens., 15, 2241–2244, 1993.

Langner, A. and Siegert, F.: Spatiotemporal fire occurrence in Borneo over a period of 10 yr, Glob. Change Biol., 15, 48–62, 2009.

Langner, A., Miettinen, J., and Siegert, F.: Land cover change 2002–2005 in Borneo and the role of fire derived from MODIS imagery, Glob. Change Biol., 13, 2329–2340, doi:10.1111/j.1365-2486.2007.01442.x, 2007.

Legg, C. A. and Laumonier, Y.: Fires in Indonesia 1997: A remote sensing perspective, Ambio, 28, 479–485, 1999.

Li, S., Goddard, L., and DeWitt, D. G.: Predictive skill of AGCM seasonal climate forecasts subject to different SST prediction methodologies, J. Climate, 21, 2169–2186, 2008.

Malingreau, J. P., Stephens, G., and Fellows, L.: Remote sensing of forest fires: Kalimantan and North Borneo in 1982–1983, Ambio, 14, 314–315, 1985.

Malingreau, J. P., Stephens, G., and Fellows, L.: Remote sensing of forest fires: Kalimantan and North Borneo in 1982–1983, Ambio, 14, 314–321 , 1995.

Miettinen, J., Shi, C., and Liew, S.: Influence of peatland and land cover distribution on fire regimes in insular Southeast Asia, Reg. Environ. Change, 11, 191–201, doi:10.1007/s10113-010-0131-7, 2011.

Mota, B. W., Pereira, J. M. C., Oom, D., Vasconcelos, M. J. P., and Schultz, M.: Screening the ESA ATSR-2 World Fire Atlas (1997–2002), Atmos. Chem. Phys., 6, 1409–1424, doi:10.5194/acp-6-1409-2006, 2006.

Naeher, L. P., Brauer, M., Lipsett, M., Zelikoff, J. T., Simpson, C. D., Koenig, J. Q., and Smith, K. R.: Woodsmoke health effects: a review, Inhal. Toxicol., 19, 67–106, 2007.

NASA: Daily TRMM and Others Rainfall Estimate (3B42 V6 derived), available at: http://gcmd.nasa.gov/records/dif_index.html, last access: 13 May 2011, 2011

NOAA: NOAA Climate Prediction Centre ENSO Indices, available at: http://www.cpc.noaa.gov/, last access: 15 August 2011, 2011a.

NOAA: NOAA Climate Prediction Centre CPC Merged Analysis of Precipitation, available at: http://www.esrl.noaa.gov/psd/data/gridded/data.cmap.html, last access: 13 May 2011, 2011b.

Page, S. E., Siegert, F., Rieley, J. O., Boehm, H.-D. V., Jaya, A., and Limin, S.: The amount of carbon released from peat and forest fires in Indonesia during 1997, Nature, 420, 61–65, 2002.

Page, S. E., Hoscilo, A., Langner, A., Tansey, K., Siegert, F., Limin, S., and Rieley, J.: Tropical peatland fires in Southeast Asia, in: Tropical Fire Ecology, edited by: Cochrane, M. Springer Berlin Heidelberg, 263–287, 2009.

Price, J. C.: Timing of NOAA afternoon passes, Int. J. Remote Sens., 12, 193–198, 1991.

Picaut J., Hackert, E., Busalacchi, A. J., and Murtugudde, R.: Mechanisms of the 1997–1998 El Niño-La Niña, as inferred from space-based observation, J. Geophys. Res., 107, 3037, doi:10.1029/2001JC000850, 2002.

R Development Core Team R: A Language and Environment for Statistical Computing, R Foundation for Statistical Computing, available at: http://www.R-project.org, last access: 30 December 2011.

Ramonet, M., Kazand, V., and Ryall, D.: A burning question, Can recent growth rate anomalies in the greenhouse gases be attributed to large-scale biomass burning events?, Atmos. Environ., 39, 2513–2517, 2005.

Roads, J. O., Chen, S.-C., and Fujioka, F.: ECPC's Weekly to Seasonal Global Forecasts, B. Am. Meteorol. Soc., 82, 639–658, 2001.

Roads, J. O., Fujioka, F., Chen, S., and Burgan, R.: Seasonal fire danger forecasts for the USA, Int. J. Wildland Fire, 14, 1–18,

doi:10.1071/WF03052, 2005.

Robel, J.: NOAA KLM Users Guide, available at: http://www.ncdc.noaa.gov/oa/pod-guide/ncdc/docs/intro.htm, last access: 30 December 2011, 2009.

Roberts, G., Wooster, M. J., and Lagoudakis, E.: Annual and diurnal african biomass burning temporal dynamics, Biogeosciences, 6, 849–866, doi:10.5194/bg-6-849-2009, 2009.

Robinson, J. M.: Fire from space: global fire evaluation using infrared remote sensing, Int. J. Remote Sens., 12, 3–24, 1991.

Sarachik, E. S. and Cane, M. A.: The El Niño-Southern Oscillation Phenomenon, Cambridge University Press, Cambridge, 364pp., 2010.

Schroeder, W., Csiszar, I., and Morisette, J.: Quantifying the impact of cloud obscuration on remote sensing of active fires in the Brazilian Amazon, Remote Sens. Environ., 112, 456–470, doi:10.1016/j.rse.2007.05.004, 2007.

Schultz, M. G.: On the use of ATSR fire count data to estimate the seasonal and interannual variability of vegetation fire emissions, Atmos. Chem. Phys., 2, 387–395, doi:10.5194/acp-2-387-2002, 2002.

Schultz, M. G., Heil, A., Hoelzemann, J. J., Spessa, A., Thonicke, K., Goldammer, J. G. A., Held, H., Pereira, J. M. C., and van het Bolscher, M.: Global wildland fire emissions from 1960 to 2000, Global Biogeochem. Cy., 22, GB2002, doi:10.1029/2007GB003031, 2008.

Siegert, F. and Hoffmann, A. A.: The 1998 forest fires in East Kalimantan (Indonesia): A quantitative evaluation using high resolution, multitemporal ERS-2 SAR images and NOAA-AVHRR hotspot data, Remote Sens. Environ., 72, 64–77, doi:10.1016/S0034-4257(99)00092-9, 2000.

Siegert, F., Ruecker, G., Hinrichs, A., and Hoffmann, A. A.: Increased damage from fires in logged forests during droughts caused by El Niño, Nature, 414, 437–440, 2001.

Simard, A. J., Haines, D. A., and Main, W. A.: Relations between El Niño/Southern Oscillation anomalies and wild land fire activity in the United States, Agr. Forest Meteorol., 36, 93–104, 1985.

Simmonds, P. G., Manning, A. J., Derwent, R. G., Ciais, P., Stenseth, N. C., Ottersen, G., Hurrell, J. W., Mysterud, A., Stolle, F., Dennis, R. A., Kurniwan. I., and Lambin. E. F.: Evaluation of remote sensing-based active fire datasets in Indonesia, Int. J. Remote Sens., 25, 471–479, 2004.

Simmonds, P. G., Manning, A. J., Derwent, R. G., Ciais, P., Ramonet, M., Kazan, V., and Ryall, D.: A burning question: Can recent growth rate anomalies in the greenhouse gases be attributed to large-scale biomas burning events?, Atmos. Environ., 39, 2513–2517, 2005.

Smith, T. M. and Reynolds, R. W.: Extended reconstruction of global sea surface temperatures based on COADS data (1854–1997), J. Climate, 16, 1495–1510, 2003.

Stenseth, N. C., Mysterud, A., Ottersen, G., Hurrell, J. W., Chan, K. S., and Lima, M.: Ecological effects of climate fluctuations, Science, 297, 1292–1996, 2002.

Stolle, F., Dennis, R. A., Kurniwan, I., and Lambin, E. F.: Evaluation of remote sensing-based active fire datasets in Indonesia, Int. J. Remote Sens., 25, 471–479, 2004.

Swetnam, T. W. and Betancourt, J. L.: Fire-Southern Oscillation relations in the Southwestern United States, Science, 24, 1017–1020, 1990.

Swetnam, T. W. and Betancourt, J. L.: Mesoscale disturbance and ecological response to decadal climate variability in the American Southwest, J. Climate, 11, 3128–3147, 1998.

Tapper, N.: Atmospheric Issues for Fire Management in Eastern Indonesia and Northern Australia, ACIAR Proceedings, 91, Fire and Sustainable Agricultural and Forestry Development in Eastern Indonesia and Northern Australia, Proceedings of an international workshop held at Northern Territory University, Darwin, Australia, 13–15 April 1999, 21–30, 1999.

Trenberth, K. and Hoar, T. J.: The 1990–1995 El Niño-Southern Oscillation Event: Longest on Record, Geophys. Res. Lett., 23, 57–60, doi:10.1029/95GL03602, 2006.

van der Werf, G. R., Randerson, J. T., Giglio, L., Collatz, G. J., Kasibhatla, P. S., and Arellano Jr., A. F.: Interannual variability in global biomass burning emissions from 1997 to 2004, Atmos. Chem. Phys., 6, 3423–3441, doi:10.5194/acp-6-3423-2006, 2006.

van der Werf, G. R., Dempewolf, J., Trigg, S. N. , Randerson, J. T., Kasibhatlae, P. S., Giglio, L., Murdiyarsog, D., Petersh, W., Mortonb, D. C., Collatz, G. J., Dolmana, A. J., and DeFries, R. S.: Climate regulation of fire emissions and deforestation in equatorial Asia, PNAS, 105, 20350–20355, doi:10.1073/pnas.0803375105, 2008.

van der Werf, G. R., Randerson, J. T., Giglio, L., Collatz, G. J., Mu, M., Kasibhatla, P. S., Morton, D. C., DeFries, R. S., Jin, Y., and van Leeuwen, T. T.: Global fire emissions and the contribution of deforestation, savanna, forest, agricultural, and peat fires (1997–2009), Atmos. Chem. Phys., 10, 11707–11735, doi:10.5194/acp-10-11707-2010, 2010.

van Nieuwstadt, M. G. L. and Sheil, D.: Drought, fire and tree survival in a Borneo rain forest, East Kalimantan, Indonesia, J. Ecol., 93, 191–201, 2005.

Walsh, R. P. D.: Drought frequency changes in Sabah and adjacent parts of northern Borneo since the late nineteenth century and possible implications for tropical rainforest dynamics, J. Trop. Ecol., 12, 385–407, 1995.

Wolter, K. and Timlin, M. S.: Measuring the strength of ENSO – how does 1997/1998 rank?, Weather, 53, 315–324, 1998.

Woods, P.: Effects of logging, drought, and fire on structure and composition of tropical forests in Sabah, Malaysia, Biotropica, 21, 290–298, 1989.

Wooster, M. J., Richards, T., and Kidwell, K. B.: NOAA 11 AVHRR/2 – thermal channel calibration update, Int. J. Remote Sens., 16, 359–363, 1995.

Wooster, M. J., Ceccato, P., and Flasse, S. P.: Indonesian fires observed using AVHRR, Int. J. Remote Sens., 19, 383–386, 1998.

Wooster, M. J. and Strub, N.: Study of the 1997 Borneo Fires: Quantitative analysis using Global Area Coverage (GAC) satellite data, Global Biogeochem. Cy., 16, 1009, doi:10.1029/2000GB001357, 2002.

Wyrtki, K.: An estimate of equatorial upwelling in the Pacific, J. Phys. Oceanogr., 11, 1205–1214, 1981.

Xie, P. and Arkin, P. A.: Analysis of global monthly precipitation using gauge observations, satellite estimates, and numerical model predictions, J. Climate, 9, 840–858, 1996.

Xie, P. and Arkin, P. A.: Global precipitation: A 17 yr monthly analysis based on gauge observations, satellite estimates, and numerical model outputs B. Am. Meteorol. Soc., 78, 2539–2558, 1997.

Xu, W., Wooster, M. J., Roberts, G., and Freeborn, P. H.: New GOES imager algorithms for cloud and active fire detection and

fire radiative power assessment across North, South and Central America, Remote Sens. Environ., 114, 1876–1895, 2011.

Yamagata, Y., Takeuchi, W., Bagan, H., Ito, A., and Adachi, M.: Forest carbon mapping using remotely sensed disturbance history in Borneo, IEEE Earthzine, online at: www.earthzine.org/2010/09/21/, last access: 30 December 2011, 2010.

Zhukov, B., Lorenz, E., Oertel, D., Wooster, M. J., and Roberts, G.: Spaceborne detection and characterization of fires during the Bispectral Infrared Detection (BIRD) experimental small satellite mission 2001–2004, Remote Sens. Environ., 100, 29–51, 2006.